Structural Design, Synthesis, and Preliminary Biological Evaluation of Novel Dihomooxacalix[4]arene-Based Anti-tumor Agents

Lin An [1,2]*, Chan Wang [1,2], Lili Han [3], Jiadong Liu [1,2], Tonghui Huang [1,2], Youguang Zheng [1,2], Chaoguo Yan [4]* and Jing Sun [4]

[1] College of Pharmacy, Xuzhou Medical University, Xuzhou, China, [2] Jiangsu Key Laboratory of New Drug Research and Clinical Pharmacy, Xuzhou Medical University, Xuzhou, China, [3] Children's Hospital Affiliated to Zhengzhou University, Zhengzhou, China, [4] College of Chemistry and Chemical Engineering, Yangzhou University, Yangzhou, China

Calixarene and its derivatives have extensively served as promising anti-tumor agents. Previously, we have synthesized a series of calix[n]arene polyhydroxyamine derivatives (n = 4, 6, 8) and found that 5,11,17,23-tetra-*tert*-butyl-25,27-bis [N-(2-hydroxyethyl)aminocarbonylmethoxyl] calix[4]arene **(CLX-4)** displayed significant effect toward SKOV3, A549, SW1990, HeLa, Raji, and MDA-MB-231 cancer cells. In the present work, we find a replacement of calix[4]arene bone and synthesized 19 novel structurally related dihomooxacalix[4]arene amide derivatives **4A−4S** to optimize its efficacy. Their abilities to induce cytotoxicity in human lung carcinoma (A549) cells, breast cancer (MCF-7) cells, cervical cancer (HeLa) cells, hepatocellular carcinoma (HepG2) cells, as well as human umbilical vein endothelial (HUVEC) cells are evaluated *in vitro*. Encouraging results show that the majority of dihomooxacalix[4]arene amide derivatives are effective at inhibiting A549 cell proliferation with the corresponding IC_{50} ranging from 0.6 to 20.1 μM. In particular, compounds **4A**, **4D**, and **4L** explore markedly increased potency (IC_{50} value is 2.0 ± 0.5 μM, 0.7 ± 0.1 μM, and 1.7 ± 0.4 μM) over the cytotoxicity profiles of control **CLX-4**, whose IC_{50} value is 2.8 ± 0.3 μM. More interestingly, **4A** also demonstrates the perfect cytotoxic effect against MCF-7, HeLa, and HepG2 cells with IC_{50} values of 1.0 ± 0.1 μM, 0.8 ± 0.2 μM, and 2.7 ± 0.4 μM. In addition, the results proved that our synthesized **4A** has much lower toxicity (41%) to normal cells at a concentration of 10 μM than that of **4D** (90%). To reveal the mechanisms, the key indicators including the cell cycle and apoptosis are observed by the flow cytometry analysis in MCF-7 cells. The results demonstrate that both **4A** and **4D** can induce the MCF-7 cell cycle arrest in G0/G1 phase and cell apoptosis. Therefore, our finding proves that the dihomooxacalix[4]arene amide derivatives are convenient platforms for potential supramolecular anticancer agents.

Keywords: supramolecular chemotherapy, calixarene, structural optimization, dihomooxacalix[4]arene, X-ray diffraction, biological evaluation

INTRODUCTION

Supramolecules generally come from the aggregation of two or more molecules based on non-covalent bond forces (Lehn, 1988; Guo et al., 2018). They usually have hydrophobic cavities in which the guests can be embedded, such as crown ethers (Flink and Reinhoudt, 1999; Kralj et al., 2008; Yokoyama and Mizuguchi, 2019), cyclodextrins (Valle, 2004; Stella and He, 2008; Zhang Y. M. et al., 2019), calixarenes (Sun et al., 2009a,b; Böhmer, 2010), cucurbiturils (Lee et al., 2003; Kim et al., 2007; Bauer et al., 2019) and pillararenes (Hu et al., 2012; Sun et al., 2018, 2019; Chen et al., 2019; Zhang R. et al., 2019).

Among those supramolecules, calixarenes are cyclic oligomers composed of phenolic units linked by methylene in the ortho positions, which are considered to be the important class representing the third generation of host–guest supramolecular chemistry. A majority of studies on calixarenes have focused on the fields of molecular recognition due to their flexible nature of the basic moiety preferable for binding and transporting ions and neutral molecules (Ludwig and Dzung, 2002; Mutihac et al., 2011; Gómez-Machuca et al., 2014; Zadmard and Alavijeh, 2014; Patra et al., 2019). In addition, calixarenes have many other structural characteristics including the easy modification of their basic core and rim via covalent attachment to various chemical scaffolds, the limited toxicity and immune responses (Geraci et al., 2008). The above advantages make these cyclic oligomers ideal for the design of new drugs and building blocks for drug carriers in biomedical fields (Da Silva et al., 2004; Hussain et al., 2017). In this regard, calixarenes and their derivatives are currently being studied and used in a variety of medicinal applications beyond their traditional place in chemistry. They could be served as chemotherapy agent (Yousaf et al., 2015; Naseer et al., 2017; Zhou et al., 2017), including antibacterials (Soares et al., 2014; Muneer et al., 2017; Ali et al., 2018; Consoli et al., 2018), antivirals (Motornaya et al., 2006; Mourer et al., 2010), antimalarials (Shah et al., 2016), and anti-inflammatory (Granata et al., 2017) enzymatic inhibitors (Läppchen et al., 2015). Moreover, they especially can be used as anti-tumor drugs (Consoli et al., 2004; Hulíková et al., 2010; Neagu et al., 2010; Nasuhi Pur and Dilmaghani, 2014); which have gained considerable attention from us. Among these works, ureido-glycocalix[8]arene carrying N-acetyl-D-glucosamine residue groups has been reported,

which inhibited C6 glioma cell migration and proliferation with independence of the N-acetyl-D-glucosamine residues (Sansone et al., 2008; Viola et al., 2010a,b). Dings et al. worked continuously on modifications and mechanism of calix[4]arene-based anti-tumor agents, identified galectin-1 (gal-1) as the molecular target, and explored compounds PTX008, PTX013 as potent anti-tumor agents (**Figure 1**) (Dings et al., 2012a,b, 2013; Koonce et al., 2017). Excitingly, PTX008 has been in a human Phase I clinical trial. The latest study further illustrated that PTX008 was an allosteric inhibitor that inhibits Galectin-1 due to BP-ALL survival (Paz et al., 2018).

In our previous work, we synthesized calix[4]arene polyhydroxyamine derivative **CLX-4** (**Figure 1**), which has been tested as a candidate anti-tumor drug with IC_{50} value against A549, SKOV3, SW1990, Hela, Raji, and MDA-MB-231 cell lines ranging from 2.8 to 5.3 μM (An et al., 2016). **CLX-4** obviously exhibited equal cytotoxic effects to those of PTX008. This inspired us to have some structural optimizations, as shown in **Figure 2**.

In our design (**Figure 2**), one possible strategy is to find alternatives to replace the material structure of **CLX-4**. Taking into account the high structural similarity, dihomooxacalix[4]arene is the closest structurally calix[4]arene analog with only one CH_2OCH_2 unit taking the place of CH_2 bridge, which results in improved conformational flexibility and the superior geometric shapes. Dihomooxacalix[4]arene was initially reported by Gutsche et al. (1981). However, over the past several years, dihomooxacalix[4]arene macrocycles and their functional derivatives were used for ion-binding application (Marcos et al., 2006, 2014; Gaeta et al., 2012; Talotta et al., 2016; Liu et al., 2017, 2018; An et al., 2018). It would seem surprising that as yet few works are so far known about the bioactivity-based approach (Harris, 1995). Therefore, dihomooxacalix[4]arenes are a particularly promising alternative to replace the calix[4]arene as the new drug bone. The other way is to chemically modify the important functional OH-CH_2-CH_2-NH-C=O group at the lower rim of **CLX-4**, which can be expected to introduce special groups with different polarity, hydrophilicity, and compatibility, leading to screening out the optimization. Appropriate R groups can be introduced to replace the 2-hydroxyethyl group linked on the aminocarbonyl dihomooxacalix[4] arene, which probably affects the anti-tumor
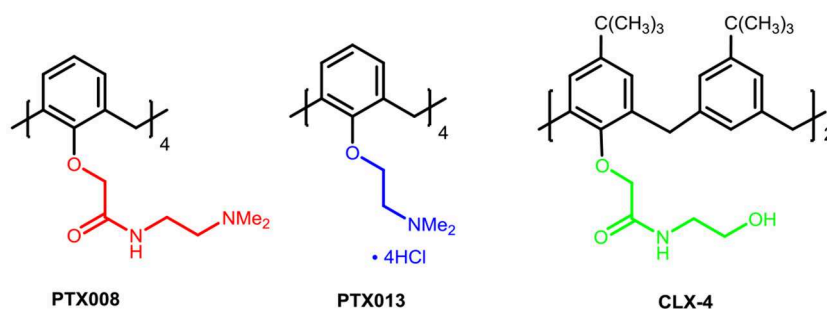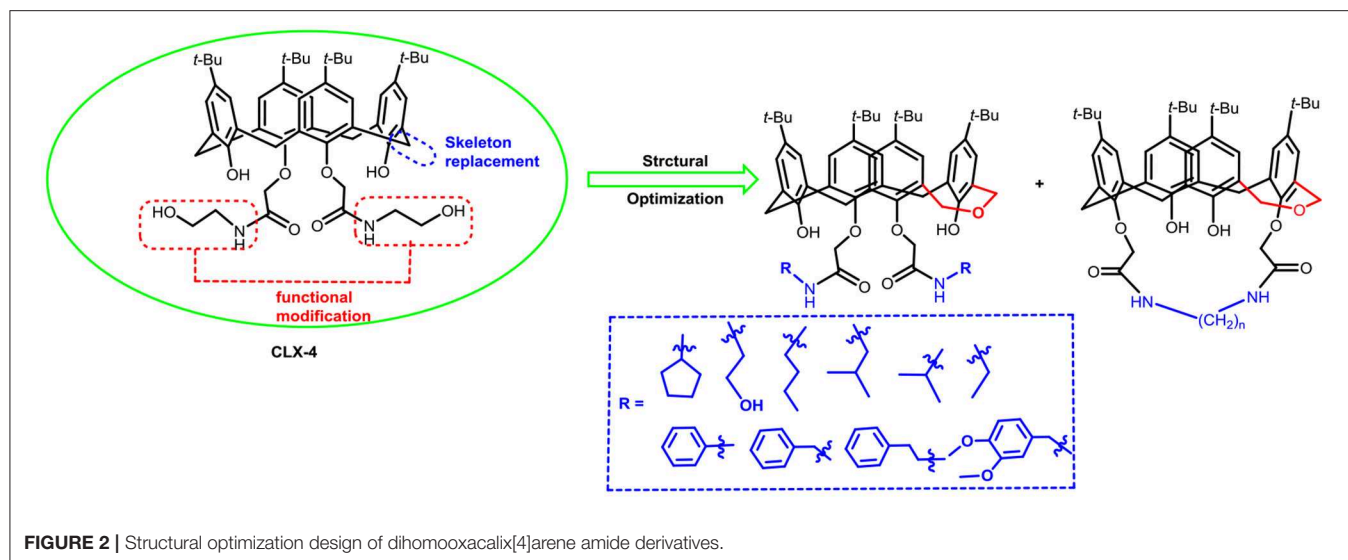

FIGURE 1 | The chemical structures of calix[4]arene-based anti-tumor agents.

FIGURE 2 | Structural optimization design of dihomooxacalix[4]arene amide derivatives.

activity by means of rigidity, electron density, flexibility, polarity and stability. To compare the influence of activity and explore the structure–activity relationship, R position attached to the acylamino unit is varied from methyl, ethyl, propyl, isopropyl, butyl, pentyl, to cyclopentyl groups, In addition, we also intend to build the spacer chains involved in the link of amino moieties on the dihomooxacalix[4]arene scaffold. As to verify our hypothesis and extend our previous work, herein we report on the synthesis, X-ray structures of a series of novel structural dihomooxacalix[4]arene amide derivatives, as well as the cell-based studies related to structure–activity relationship.

MATERIALS AND METHODS

Synthesis and Characterization

Synthesis of Dihomooxacalix[4]arene Amide Derivatives 4A–4S

p-tert-butyl dihomooxacalix[4]arenes 1 was synthesized according to Gutsche's method (Gutsche et al., 1981). All other reagents and solvents were commercially available reagents with analytical grade and used without further purification. The products were purified by recrystallization or using preparative separations in flash column chromatography. Reactions were monitored by thin-layer chromatography (TLC) on 2.5 mm Merck silica gel F254 strips. Melting points were determined with capillaries on an YRT-3 microscope apparatus and were uncorrected. All ^{1}H NMR and ^{13}C NMR spectra were recorded at 400 MHz on a Bruker AVANCE II 400 spectrometer. IR spectra were obtained on a Nicolet FT-IR 8400 spectrometer (KBr disc). High Resolution Mass Spectrometry were carried out on (UHR-TOF) maXis 4G mass spectrometer.

General Procedure for the Synthesis of Dihomooxacalix[4]arene Ester 2A

Under ultrasound irradiation, a mixture of *p-tert*-butyl dihomooxacalix[4]arene 1 (6.78 g, 10 mmol), bromoethylacetate

(6.68 ml, 60 mmol), and acetone (100 ml) was stirred at 55°C. The reaction was monitored by TLC until the start material 1 disappeared. The mixture was poured into a large amount of water and extracted with chloroform. The organic layers were collected, dried over anhydrous sodium sulfate, concentrated *in vacuo*, and further purified by silica gel column chromatography (1:4 ethyl acetate-petroleum ether) to provide the product 2A as the white solid, which was used in the next step.

General Procedure for the Synthesis of Dihomooxacalix[4]arene Amide 3A

Ester 2A (0.230 g, 0.3 mmol) was dissolved in dichloromethane (2 ml), and ethanolamine (0.037 g, 0.6 mmol) was added to the solution. Then, the resulting mixture was stirred at room temperature for 24 h. It was concentrated *in vacuo*, washing with 95% ethanol twice to give the solid precipitate, followed by filtration, purified by silica gel column chromatography (15:1 v/v, dichloromethane/methanol) to afford the desired 3A in quantitative yield.

General Procedure for the Synthesis of Dihomooxacalix[4]arene Amides 4A–4B

A solution of ester 2A (0.425 g, 0.5 mmol) and hydroxylamine (0.244 g, 4 mol) or dihydroxylamine (0.421 g, 4 mol) in refluxing ethanol/toluene (50 ml, v/v = 1:1) for 72 h. After the completion of the reaction (TLC), the solution was concentrated *in vacuo*, leaving the pale oil residue, which was washed with 95% ethanol to give the solid precipitate, followed by filtration, purified by silica gel column chromatography to yield 4A or 4B as a white solid.

General Procedure for the Synthesis of Dihomooxacalix[4]arene Amides 4C–4D

A solution of 1,4-diaminobutane or 1,6-diaminohexane (2 ml) in methanol (2 ml) kept at 0°C was added dropwise solution of ester 2A (0.425 g, 0.5 mmol) in methanol (1 ml) for 30 min. The ice

bath was removed and the reaction mixture was warmed to room temperature and stirred for 24 h. The solution was concentrated *in vacuo*, and the residue was treated with cool water to afford the pale yellow solid precipitate, further purified by silica gel flash column chromatography to yield 4C—4D.

General Procedure for the Synthesis of Bridged Dihomooxacalix[4]arene Amides 4E—4G

A mixture of ester 2A (0.425 g, 0.5 mmol) and 2 ml of ethylenediamine (or 1,4-diaminobutane, 1,6-diaminohexane) was dissolved in ethanol (5 ml) and refluxed for 24 h. When the reaction was complete, the solution was concentrated *in vacuo*, followed by dropwise distilled water was added. The crude product was extracted and filtered to give the pale yellow solid precipitate, further purified by silica gel flash column chromatography to yield compound 4E—4G.

General Procedure for the Synthesis of Dihomooxacalix[4]arene Amides 4H—4P

A solution of ethylamine hydrochloride (2 ml) in ethanol (2 ml), kept at 0°C, was added dropwise to a solution of ester 2A (0.425 g, 0.5 mmol) in ethanol (1 ml) for 30 min. Then, the mixture was stirred at room temperature overnight. After the completion of the reaction, the solvent was removed *in vacuo*, and then the residue was treated with cool water to give the solid precipitate, further purified by silica gel flash column chromatography to yield compound 4H. Compound 4I—4P was prepared by a similar procedure.

General Procedure for the Synthesis of 4Q—4S

A solution of 3A with cyclopentylamine (2 ml) was stirred for 4 h at room temperature. Then, the solution was concentrated *in vacuo* to give the crude product, followed by the purification with silica gel flash chromatography to give the compound 4Q, as white powder.

Compound **4R—4S** was prepared by a similar procedure.

7,13,19,25-tetra-*tert*-butyl-28,30-di-hydroxy-27,29-(ethoxycarbonylmethoxyl)-2,3-dihomo-3-oxacalix[4]arene (2A): White solid, m.p. 168.7–171.4°C, yield: 95.6% (**Figure S1**); ^{1}H NMR (400 MHz, CDCl$_3$) δ (ppm): 1.11, 1.19, 1.23, 1.26 (4s, 36H), 1.30 (t, 3H, J = 7.2 Hz), 1.38 (t, 3H, J = 7.2 Hz), 3.28 (d, 1H, J = 12.8 Hz), 3.37 (d, 1H, J = 13.6 Hz), 3.46 (d, 1H, J = 13.2 Hz), 4.21 (d, 1H, J = 9.2 Hz), 4.24 (dd, 1H, J_1 = 7.2 Hz, J_2 = 1.2 Hz), 4.28 (dd, 1H, J_1 = 7.2 Hz, J_2 = 1.2 Hz), 4.31 (d, 1H, J = 13.2 Hz), 4.34–4.41 (m, 3H), 4.46 (d, 1H, J = 12.8 Hz), 4.52 (d, 1H, J = 15.6 Hz), 4.67 (d, 1H, J = 10.4 Hz), 4.71 (d, 1H, J = 13.6 Hz), 4.81 (d, 1H, J = 15.6 Hz), 4.98 (d, 1H, J = 10.0 Hz), 5.35 (d, 1H, J = 9.2 Hz), 5.53 (d, 1H, J = 16.0 Hz), 6.89 (d, 1H, J = 2.4 Hz), 6.96 (d, 1H, J = 2.4 Hz), 6.99 (d, 1H, J = 2.4 Hz), 7.03 (q, 2H, J = 2.4 Hz), 7.07 (d, 1H, J = 2.8 Hz), 7.30 (s, 1H), 7.40 (d, 1H, J = 2.4 Hz), 7.77 (s, 1H); ^{13}C NMR (100 MHz, CDCl$_3$) δ (ppm): 14.3, 31.1, 31.4, 31.5, 31.6, 33.8, 34.1, 60.9, 61.4, 71.6, 72.1, 72.3, 122.6, 124.1, 125.0, 125.3, 125.4, 125.8, 126.0, 126.9, 127.6, 127.7, 128.2, 129.5, 129.8, 132.3, 132.7, 133.7, 141.1, 142.0, 146.5,

147.5, 149.4, 150.1, 152.9, 155.0, 168.8, 170.5; IR (KBr, cm^{-1}) ν 3313, 2959, 2868, 1665, 1483, 1364, 1298, 876.

7,13,19,25-tetra-*tert*-butyl-28,30-di-hydroxy-27-(ethoxycarbonylmethoxyl)-29-(N-(2-hydroxyethyl) amino carbonyl methoxyl)-2,3-dihomo-3-oxacalix[4]arene (3A): White solid, yield: 85.1%, m.p. 188.6–191.8°C (**Figure S2**); ^{1}H NMR (400 MHz, CDCl$_3$) δ (ppm): 1.14, 1.22, 1.26 (3s, 36H), 1.33 (t, 3H, J = 7.2 Hz), 3.36 (d, 1H, J = 13.6 Hz), 3.42 (d, 1H, J = 13.2 Hz), 3.49 (d, 1H, J = 13.2 Hz), 3.67–3.87 (m, 4H), 4.14 (d, 1H, J = 13.2 Hz), 4.20 (d, 1H, J = 9.2 Hz), 4.24–4.35 (m, 4H), 4.39 (d, 1H, J = 15.6 Hz), 4.47 (d, 2H, J = 13.6 Hz), 4.64 (d, 1H, J = 16.0 Hz), 4.76 (d, 1H, J = 15.2 Hz), 4.94 (d, 1H, J = 9.6 Hz), 5.08–5.13 (m, 2H), 6.91 (d, 1H, J = 2.4 Hz), 6.98 (d, 1H, J = 2.4 Hz), 7.00 (d, 1H, J = 2.4 Hz), 7.10–7.12 (q, 3H, J = 2.4 Hz), 7.23 (d, 1H, J = 2.0 Hz), 7.43(d, 1H, J = 2.4 Hz), 7.77 (s, 1H), 8.85 (t, 1H, J = 5.2 Hz; ^{13}C NMR (100 MHz, CDCl$_3$) δ (ppm): 14.2, 30.8, 30.9, 31.0, 31.1, 31.3, 31.5, 31.6, 31.7, 32.1, 33.8, 33.9, 34.2, 42.8, 61.4, 62.8, 71.3, 71.9, 72.3, 74.1, 122.8, 124.5, 125.3, 125.4, 125.8, 126.2, 126.4, 127.1, 128.0, 128.1, 129.1, 129.6, 131.7, 132.7, 133.9, 142.4, 143.0, 147.5, 147.8, 148.9, 149.7, 152.0, 154.4, 170.1, 170.3; IR (KBr, cm^{-1}) ν 3433, 2961, 2868, 1757, 1670, 1485, 1209, 1065, 874; MS (m/z): HRMS (ESI) Calcd for C$_{53}$H$_{71}$NNaO$_9$ ([M+Na]$^+$): 888.5021, found: 888.5029.

7,13,19,25-tetra-*tert*-butyl-28,30-di-hydroxy-27,29-di-(N-(2-hydroxyethyl)-aminocarbonylmethoxyl)-2,3-dihomo-3-oxacalix[4]arene (4A): White solid, m.p. 139.7–142.3°C, yield: 87.2% (**Figure S3**); ^{1}H NMR (400 MHz, CDCl$_3$) δ (ppm) 1.03, 1.20, 1.26, 1.29 (4s, 36H), 3.44–3.53 (m, 5H), 3.59–3.64 (m, 2H), 3.79 (s, 4H), 4.17–4.29 (m, 4H), 4.38 (d, 1H, J = 10.0 Hz), 4.54 (dd, 1H, J_1 = 15.2 Hz, J_2 = 5.2 Hz), 4.60–4.68 (m, 4H), 4.84 (d, 1H, J = 10.0 Hz), 6.85 (d, 1H, J = 1.6 Hz), 6.92 (d, 1H, J = 2.4 Hz), 7.02 (d, 2H, J = 2.0 Hz), 7.16 (d, 1H, J = 2.0 Hz), 7.22 (d, 1H, J = 2.0 Hz), 7.24 (d, 1H, J = 2.0 Hz), 7.31 (s, 1H), 7.38 (d, 2H, J = 2.4 Hz), 8.78 (t, 1H, J = 5.2 Hz), 8.84 (t, 1H, J = 5.2 Hz); ^{13}C NMR (100 MHz, CDCl$_3$) δ (ppm): 31.0, 31.2, 31.4, 31.5, 31.9, 34.0, 34.1, 34.2, 42.5, 62.0, 62.2, 70.8, 72.1, 73.9, 74.4, 76.7, 77.0, 77.2, 77.3, 122.7, 124.7, 125.9, 126.0, 126.3, 127.1, 127.4, 127.7, 127.8, 128.0, 128.8, 129.3, 131.9, 132.1, 133.6, 143.1, 143.8, 148.1, 148.4, 148.8, 149.9, 151.2, 152.6, 169.4, 169.7; IR (KBr, cm^{-1}) ν 3389, 3366, 2959, 2870, 1666, 1545, 1485, 1447, 1362, 874; MS (m/z): HRMS (ESI) Calcd for C$_{53}$H$_{72}$N$_2$NaO$_9$ ([M+Na]$^+$): 903.5130, found: 903.5145.

7,13,19,25-tetra-*tert*-butyl-28,30-di-hydroxy-27,29-di-(N,N-bis(2-hydroxyethyl)-aminocarbonylmethoxyl)-2,3-dihomo—3-oxacalix[4]arene (4B): White solid, m.p. 210.7–212.5°C, yield: 86.7% (**Figure S4**); ^{1}H NMR (400 MHz, DMSO-d_6) δ (ppm): 1.11, 1.18, 1.20, 1.24 (4s, 36H), 3.42–3.49 (m, 6H), 3.54–3.62 (m, 10H), 3.67 (s, 2H), 3.87–3.91 (m, 1H), 4.19 (d, 1H, J = 9.2 Hz), 4.26 (d, 1H, J = 10.0 Hz), 4.36 (dd, 2H, J_1 = 12.8 Hz, J_2 = 6.0 Hz), 4.56 (d, 1H, J = 12.8 Hz), 4.66 (d, 2H, J = 13.2 Hz), 4.74 (d, 2H, J = 9.2 Hz), 4.78 (s, 1H), 4.90 (s, 1H), 4.97 (s, 1H), 5.03 (s, 1H), 5.06 (d, 1H, J = 4.8 Hz), 5.32 (d, 1H, J = 13.2 Hz), 6.89 (d, 1H, J = 2.4 Hz), 7.00 (d, 1H, J = 2.0 Hz), 7.02 (d, 1H, J = 2.0 Hz), 7.13 (s, 1H), 7.16 (s, 1H), 7.22 (d, 1H, J = 2.0 Hz), 7.36 (d, 1H, J = 2.0 Hz), 7.48 (d, 1H, J = 2.0 Hz), 7.71 (s, 1H), 8.61 (s, 1H); ^{13}C NMR (100 MHz, DMSO-d_6) δ (ppm): 31.4, 31.6, 31.8, 31.9, 34.0, 34.3, 59.1, 122.8, 125.5, 125.7, 126.6,

126.7, 127.2, 127.9, 129.8, 132.9, 133.4, 134.5, 140.8, 141.0, 146.0, 146.7, 150.0, 152.1, 152.4, 155.3, 169.3, 169.6; IR (KBr, cm^{-1}) ν 3389, 3045, 2957, 2870, 1643, 1485, 1443, 1364, 876; MS (m/z): HRMS (ESI) Calcd for C$_{57}$H$_{80}$N$_2$NaO$_{11}$ ([M+Na]$^+$): 991.5654, found: 991.5674.

7,13,19,25-tetra-*tert*-butyl-28,30-di-hydroxy-27,29-di-(N-(4-aminobutyl)-aminocarbonylmethoxyl)-2,3-dihomo-3-oxacalix[4] arene (4C): White solid, m.p. 129.4–131.2°C, yield: 96.2% (**Figure S5**); ^{1}H NMR (400 MHz, CDCl$_3$) δ (ppm): 1.16, 1.24, 1.25, 1.27 (4s, 36H), 1.32 (d, 2H, J = 11.2 Hz), 1.40–1.43 (m, 2H), 1.45–1.53 (m, 3H), 1.57–1.73 (m, 4H), 2.57 (t, 2H, J = 7.2 Hz), 2.68 (t, 2H, J = 6.8 Hz), 3.18–3.26 (m, 2H), 3.43 (t, 2H, J = 12.0 Hz), 3.52–3.66 (m, 3H), 4.10 (d, 1H, J = 13.6 Hz), 4.16–4.22 (m, 2H), 4.35 (s, 1H), 4.38–4.40 (m, 2H), 4.44 (d, 1H, J = 9.2 Hz), 4.50 (d, 1H, J = 11.2 Hz), 4.58 (d, 1H, J = 10.0 Hz), 4.80 (dd, 2H, J_1 = 19.2 Hz, J_2 = 15.2 Hz), 4.96 (d, 1H, J = 10.4 Hz), 6.87 (d, 1H, J = 2.4 Hz), 7.01 (d, 1H, J = 2.4 Hz), 7.04 (d, 1H, J = 2.0 Hz), 7.14 (d, 1H, J = 2.4 Hz), 7.16 (d, 1H, J = 2.4 Hz), 7.23 (t, 2H, J = 2.4 Hz), 7.46 (d, 1H, J = 2.4 Hz), 8.24 (s, 1H), 8.74 (t, 1H, J = 4.2 Hz), 9.00 (t, 1H, J = 4.2 Hz); ^{13}C NMR (100 MHz, CDCl$_3$) δ (ppm): 26.4, 26.9, 31.0, 31.1, 31.3, 31.5, 32.4, 33.9, 34.0, 34.3, 39.2, 39.5, 41.9, 42.0, 71.2, 71.9, 73.8, 74.5, 122.2, 124.4, 125.7, 126.0, 126.9, 127.0, 127.2, 127.3, 127.4, 127.6, 128.6, 129.6, 131.5, 132.4, 133.8, 143.0, 143.7, 148.0, 148.6, 148.9, 149.5, 151.4, 153.2, 168.0, 168.5; IR (KBr, cm^{-1}) ν 3369, 3194, 2959, 2866, 1674, 1483, 1296, 874; MS (m/z): HRMS (ESI) Calcd for C$_{57}$H$_{83}$N$_4$O$_7$ ([M+H]$^+$): 935.6256, found: 935.6284.

7,13,19,25-tetra-*tert*-butyl-28,30-di-hydroxy-27,29-di-(N-(6-aminohexyl)-aminocarbonylmethoxyl)-2,3-dihomo-3-oxacalix[4] arene (4D): White solid, m.p. 123.3–125.9°C, yield: 63.3% (**Figure S6**); ^{1}H NMR (400 MHz, CDCl$_3$) δ (ppm): 1.18 (s, 9H), 1.27 (brs, 18H), 1.29 (s, 9H), 1.33 (d, 10H, J = 12.0 Hz), 1.57–1.69 (m, 5H), 1.99 (d, 2H, J = 3.6 Hz), 2.52–2.55 (m, 2H), 2.60–2.63 (m, 2H), 2.70 (t, 1H, J = 7.2 Hz), 3.17–3.28 (m, 3H), 3.42–3.68 (m, 6H), 4.11 (d, 1H, J = 13.6 Hz), 4.16–4.23 (m, 2H), 4.37 (s, 1H), 4.40–4.44 (m, 2H), 4.49 (d, 1H, J = 14.8 Hz), 4.62 (d, 1H, J = 9.6 Hz), 4.80 (t, 2H, J = 15.2 Hz), 4.96 (d, 1H, J = 10.4 Hz), 6.89 (d, 1H, J = 2.0 Hz), 7.04 (d, 1H, J = 2.0 Hz), 7.05 (d, 1H, J = 2.4 Hz), 7.16 (d, 1H, J = 2.0 Hz), 7.18 (d, 1H, J = 2.0 Hz), 7.22–7.24 (m, 2H), 7.48 (d, 1H, J = 2.4 Hz), 8.24 (s, 1H), 8.70 (t, 1H, J = 5.6 Hz), 8.96 (t, 1H, J = 6.0 Hz); ^{13}C NMR (100 MHz, CDCl$_3$) δ (ppm): 26.5, 26.9, 27.0, 29.5, 31.1, 31.3, 31.5, 33.6, 33.9, 34.3, 42.0, 42.1, 122.3, 124.4, 127.2, 127.4, 128.6, 131.5, 132.3, 133.7, 142.9, 148.6, 148.9, 151.5, 153.2, 167.9, 168.4; IR (KBr, cm^{-1}) ν 3350, 3215, 2957, 2862, 1674, 1483, 1298, 818; MS (m/z): HRMS (ESI) Calcd for C$_{61}$H$_{91}$N$_4$O$_7$ ([M+H]$^+$): 991.6882, found: 991.6883.

7,13,19,25-tetra-*tert*-butyl-28,30-di-hydroxy-27,29-N,N-(ethane-1,2-diyl)-aminocarbonylmethoxyl)-2,3-dihomo-3-oxacalix[4] arene (4E): White solid, m.p. 204.8–206.3°C, yield: 86.6% (**Figure S7**); ^{1}H NMR (400 MHz, CDCl$_3$) δ (ppm): 1.16, 1.24, 1.25, 1.26 (4s, 36H), 3.10–3.23 (m, 2H), 3.40 (dd, 2H, J_1 = 13.2 Hz, J_2 = 2.8 Hz), 3.58 (d, 1H, J = 13.6 Hz), 4.01 (d, 1H, J = 13.6 Hz), 4.14–4.22 (m, 3H), 4.24 (d, 1H, J = 9.6 Hz), 4.28 (d, 1H, J = 14.0 Hz), 4.38–4.46 (m, 3H), 4.67 (d, 1H, J = 14.4 Hz), 4.74–4.80 (m, 2H), 4.89 (d, 1H, J = 9.6 Hz), 6.89 (d, 1H, J = 2.4 Hz), 7.02 (dd, 2H, J_1 = 4.0 Hz, J_2 = 2.4 Hz), 7.08 (d, 1H, J

= 2.4 Hz), 7.13 (d, 2H, J = 3.2 Hz), 7.25 (s, 1H), 7.28 (d, 1H, J = 2.4 Hz), 7.53, 8.11 (2s, 2H), 8.30–8.33 (m, 1H), 8.60–8.63 (m, 1H); ^{13}C NMR (100 MHz, CDCl$_3$) δ (ppm): 29.5, 30.5, 31.2, 31.3, 31.5, 32.6, 33.9, 34.3, 39.2, 39.6, 71.3, 72.8, 73.7, 74.0, 122.6, 124.4, 125.9, 126.1, 126.2, 126.4, 126.8, 127.1, 127.8, 128.0, 128.9, 129.6, 131.4, 131.9, 143.0, 143.1, 147.5, 147.8, 148.7, 149.1, 151.9, 152.2, 167.8, 168.7; IR (KBr, cm^{-1}) ν 3373, 3180, 3049, 2961, 2868, 1692, 1530, 1483, 1364, 1296, 874; MS (m/z): HRMS (ESI) Calcd for C$_{51}$H$_{66}$N$_2$NaO$_7$ ([M+Na]$^+$): 841.4762, found: 841.4771.

7,13,19,25-tetra-*tert*-butyl-28,30-di-hydroxy-27,29-N,N-(propane-1,3-diyl)-aminocarbonylmethoxyl)-2,3-dihomo-3-oxacalix[4] arene (4F): White solid, m.p. 189.5–191.4°C, yield: 92.0%; (**Figure S8**) ^{1}H NMR (400 MHz, CDCl$_3$) δ (ppm): 1.16, 1.24, 1.25, 1.26 (4s, 36H), 2.29–2.38 (m, 2H), 3.26 (s, 2H), 3.42 (dd, 2H, J_1 = 12.4 Hz, J_2 = 1.2 Hz), 3.57 (d, 1H, J = 13.6 Hz), 3.66 (d, 1H, J = 14.8 Hz), 3.76 (d, 1H, J = 16.8 Hz), 4.05 (d, 1H, J = 14.0 Hz), 4.15 (d, 1H, J = 13.2 Hz), 4.21–4.26 (m, 2H), 4.31 (d, 1H, J = 12.8 Hz), 4.36–4.22 (m, 2H), 4.70–4.74 (m, 2H), 4.80–4.87 (m, 2H), 6.90 (s, 1H), 7.03 (s, 2H), 7.13 (d, 2H, J = 13.2 Hz), 7.32 (s, 1H), 7.50 (s, 1H), 8.16 (s, 1H), 8.50 (s, 1H), 8.69 (s, 1H); ^{13}C NMR (100 MHz, CDCl$_3$) δ (ppm): 23.2, 30.0, 31.1, 31.3, 31.5, 32.3, 33.9, 34.3, 36.1, 71.0, 72.4, 73.8, 74.0, 122.7, 124.7, 125.9, 126.2, 126.3, 126.5, 126.8, 126.9, 127.5, 128.0, 129.1, 129.6, 131.2, 131.9, 133.7, 143.1, 143.3, 148.0, 148.2, 148.7, 149.1, 151.8, 152.6, 168.2, 169.3; IR (KBr, cm^{-1}) ν 3377, 3049, 2961, 2868, 1690, 1599, 1483, 1443, 1298, 874; MS (m/z): HRMS (ESI) Calcd for C$_{52}$H$_{68}$N$_2$NaO$_7$ ([M+Na]$^+$): 855.4919, found: 855.4922.

7,13,19,25-tetra-*tert*-butyl-28,30-di-hydroxy-27,29-27,29-N,N-(butane-1,4-diyl)–aminocarbonylmethoxyl)-2,3-dihomo-3-oxacalix[4] arene (4G): White solid, m.p. 157.6–158.7°C, yield: 91.9% (**Figure S9**); ^{1}H NMR (400 MHz, DMSO-d_6) δ (ppm): 1.09, 1.19, 1.22, 1.23 (4s, 36H), 1.63 (d, 4H, J = 4.4 Hz), 3.42–3.52 (m, 6H), 4.21 (d, 1H, J = 9.6 Hz), 4.27–4.34 (m, 4H), 4.36–4.42 (m, 4H), 4.54 (d, 1H, J = 14.0 Hz), 4.73 (d, 1H, J = 9.6 Hz), 4.79 (d, 1H, J = 10.0 Hz), 6.92 (d, 1H, J = 2.0 Hz), 7.04 (d, 2H, J = 2.4 Hz), 7.22 (d, 1H, J = 2.0 Hz), 7.26 (s, 1H), 7.28 (s, 1H), 7.32 (d, 1H, J = 2.4 Hz), 7.41 (d, 1H, J = 2.0 Hz), 7.58 (d, 1H, J = 2.0 Hz), 7.98 (s, 1H), 8.20 (t, 1H, J = 6.4 Hz), 8.35 (t, 1H, J = 6.0 Hz); ^{13}C NMR (100 MHz, CDCl$_3$) δ (ppm): 25.0, 25.4, 30.3, 31.0, 31.1, 31.3, 31.5, 31.6, 31.9, 33.9, 34.3, 38.4, 70.9, 72.5, 74.1, 74.5, 122.9, 124.6, 125.8, 126.1, 126.5, 126.6, 126.7, 127.0, 128.0, 128.7, 129.6, 131.2, 131.6, 133.8, 143.0, 143.2, 147.8, 148.4, 149.0, 149.4, 151.8, 153.0, 168.1, 169.0; IR (KBr, cm^{-1}) ν 3369, 3389, 3233, 3194, 3049, 2961, 2868, 1686, 1535, 1485, 1298, 874; MS (m/z): HRMS (ESI) Calcd for C$_{53}$H$_{70}$N$_2$NaO$_7$ ([M+Na]$^+$): 869.5075, found: 869.5082.

7,13,19,25-tetra-*tert*-butyl-28,30-di-hydroxy-27,29-di-(N-ethyl-aminocarbonylmethoxyl)-2,3-dihomo-3-oxacalix[4]arene (4H): White solid, m.p. 138.9–141.2°C, yield: 87.2% (**Figure S10**); ^{1}H NMR (400 MHz, CDCl$_3$) δ (ppm): 1.16 (s, 9H), 1.24 (t, 6H, J = 14.6 Hz), 1.25 (brs, 18H), 1.27 (s, 9H), 3.32–3.39 (m, 2H), 3.45 (t, 2H, J = 12.8 Hz), 3.53 (q, 2H, J = 6.8 Hz), 3.61 (q, 1H, J = 6.4 Hz), 4.14 (dd, 2H, J_1 = 18.8 Hz, J_2 = 13.6 Hz), 4.22 (d, 1H, J = 10.4 Hz), 4.33 (d, 1H, J = 13.2 Hz), 4.38–4.45 (m, 2H), 4.52 (d, 1H, J = 15.2 Hz), 4.64 (d, 1H, J = 10.0 Hz), 4.72 (dd, 2H, J_1 = 18.0 Hz, J_2 = 2.0 Hz), 4.89 (d, 1H, J = 10.0 Hz), 6.89 (d, 1H, J = 2.0 Hz), 7.02 (d, 1H, J = 1.6 Hz), 7.05 (d, 1H,

J = 2.0 Hz), 7.17 (dd, 2H, J_1 = 7.6 Hz, J_2 = 2.0 Hz), 7.22 (dd, 2H, J_1 = 10.4 Hz, J_2 = 2.0 Hz), 7.45 (d, 1H, J = 2.0 Hz), 7.59 (s, 1H), 8.17 (s, 1H), 8.75 (t, 1H, J = 5.2 Hz), 8.93 (t, 1H, J = 5.6 Hz); ^{13}C NMR (100 MHz, CDCl$_3$) δ (ppm): 14.1, 14.8, 31.1, 31.2, 31.3, 31.5, 32.2, 33.9, 34.0, 34.2, 34.3, 34.4, 71.0, 72.0, 74.6, 122.3, 124.7, 125.7, 125.9, 126.2, 126.8, 127.2, 127.3, 127.4, 127.7, 128.8, 129.6, 131.5, 132.4, 133.7, 142.9, 143.7, 148.1, 148.6, 148.9, 149.5, 151.5, 153.1, 167.9, 168.3; IR (KBr, cm^{-1}) ν 3350, 3244, 2961, 2870, 1682, 1485, 874; MS (m/z): HRMS (ESI) Calcd for C$_{53}$H$_{72}$N$_2$NaO$_7$ ([M+Na]$^+$): 871.5232, found: 871.5249.

7,13,19,25-tetra-*tert*-butyl-28,30-di-hydroxy-27,29-di-(N-isopropyl-aminocarbonylmethoxyl)-2,3-dihomo-3-oxacalix[4]arene (4I): White solid, m.p. 133.3–135.7°C, yield: 76.3% (**Figure S11**); ^{1}H NMR (400 MHz, CDCl$_3$) δ (ppm): 1.16 (s, 9H), 1.20 (d, 4H, J = 6.4 Hz), 1.25 (brs, 18H), 1.29 (s, 9H), 1.31 (d, 8H, J = 4.8 Hz), 3.41 (t, 2H, J = 14.8 Hz), 3.57 (d, 1H, J = 13.6 Hz), 4.11 (d, 1H, J = 13.6 Hz), 4.18–4.47 (m, 8H), 4.55 (d, 1H, J = 10.4 Hz), 4.77 (dd, 2H, J_1 = 18.8 Hz, J_2 = 15.6 Hz), 4.99 (d, 1H, J = 10.4 Hz), 6.85 (s, 1H), 7.03 (d, 2H, J = 14.4 Hz), 7.15 (s, 2H), 7.23 (d, 2H, J = 4.0 Hz), 7.45 (s, 1H), 7.61 (s, 1H), 7.90 (s, 1H), 8.79 (dd, 2H, J_1 = 19.6 Hz, J_2 = 7.6 Hz); ^{13}C NMR (100 MHz, CDCl$_3$) δ (ppm): 22.0, 22.3, 22.6, 31.1, 31.3, 31.5, 31.6, 33.9, 34.2, 41.4, 41.5, 71.0, 71.8, 74.2, 74.6, 121.9, 123.9, 125.6, 125.8, 126.1, 127.0, 127.4, 127.5, 127.6, 128.5, 129.7, 131.8, 132.4, 133.8, 142.8, 143.5, 147.7, 148.4, 149.0, 150.3, 151.3, 153.8, 167.4, 167.9; IR (KBr, cm^{-1}) ν 3340, 2962, 2870, 1682, 1485, 1460, 874; MS (m/z): HRMS (ESI) Calcd for C$_{55}$H$_{76}$N$_2$NaO$_7$ ([M+Na]$^+$): 899.5545, found: 899.5562.

7,13,19,25-tetra-*tert*-butyl-28,30-di-hydroxy-27,29-di-(N-isobutyl-aminocarbonylmethoxyl)-2,3-dihomo-3-oxacalix[4]arene (4J): White solid, m.p. 128.1–130.8°C, yield: 86.5% (**Figure S12**); ^{1}H NMR (400 MHz, CDCl$_3$) δ (ppm): 0.90–0.98 (m, 12H), 1.16 (s, 9H), 1.24 (brs, 18H), 1.26 (s, 9H) 1.85 (s, 1H), 1.99 (s, 1H), 2.94–3.04 (m, 2H), 3.38–3.46 (m, 3H), 3.56 (d, 2H, J = 13.6 Hz), 4.08 (d, 1H, J = 15.2 Hz), 4.21 (d, 2H, J = 12.4 Hz), 4.35–4.48 (m, 4H), 4.59 (d, 1H, J = 10.4 Hz), 4.75–4.84 (m, 2H), 4.96 (d, 1H, J = 10.4 Hz), 6.85 (s, 1H), 7.02 (d, 2H, J = 6.0 Hz), 7.14 (d, 2H, J = 11.2 Hz), 7.21 (s, 2H), 7.47 (d, 2H, J = 14.4 Hz), 8.09 (s, 1H), 8.62 (s, 1H), 8.94 (s, 1H); ^{13}C NMR (100 MHz, CDCl$_3$) δ (ppm): 20.4, 20.5, 28.5, 31.1, 31.3, 31.5, 33.9, 34.2, 34.3, 46.8, 47.0, 71.2, 72.0, 73.9, 74.5, 122.1, 124.2, 125.5, 125.9, 126.0, 126.9, 127.0, 127.2, 127.3, 127.4, 127.6, 128.6, 129.6, 131.7, 132.3, 133.8, 142.8, 143.4, 147.8, 148.5, 148.8, 149.5, 151.5, 153.2, 168.0, 168.6; IR (KBr, cm^{-1}) ν 3350, 3194, 2961, 2870, 1680, 1483, 1364; MS (m/z): HRMS (ESI) Calcd for C$_{57}$H$_{80}$N$_2$NaO$_7$ ([M+Na]$^+$): 927.5858, found: 927.5873.

7,13,19,25-tetra-*tert*-butyl-28,30-di-hydroxy-27,29-di-(N-butyl-aminocarbonylmethoxyl)-2,3-dihomo-3-oxacalix[4]arene (4K): White solid, m.p. 119.5–120.8°C, yield: 91.9% (**Figure S13**); ^{1}H NMR (400 MHz, CDCl$_3$) δ (ppm): 0.84 (t, 3H, J = 7.2 Hz), 0.92 (t, 3H, J = 7.2 Hz), 1.17 (s, 9H), 1.25 (brs, 18H), 1.28 (s, 9H) 1.32–1.43 (m, 4H), 1.56–1.71 (m, 4H), 3.19–3.31 (m, 2H), 3.44 (t, 2H, J = 14.0 Hz), 3.50–3.57 (m, 2H), 3.61–3.66 (m, 1H), 4.11 (d, 1H, J = 13.2 Hz), 4.17–4.24 (m, 2H), 4.35–4.42 (m, 3H), 4.49 (d, 1H, J = 15.2 Hz), 4.63 (d, 1H, J = 10.0 Hz), 4.76 (dd, 2H, J_1 = 18.8 Hz, J_2 = 15.2 Hz), 4.93 (d, 1H, J = 10.4 Hz), 6.88 (d, 1H, J = 2.0 Hz), 7.04 (dd, 2H, J_1 = 11.2 Hz, J_2 = 1.6 Hz), 7.16

(dd, 2H, J_1 = 8.4 Hz, J_2 = 1.6 Hz), 7.23 (dd, 2H, J_1 = 6.4 Hz, J_2 = 1.6 Hz), 7.46 (d, 1H, J = 2.0 Hz), 7.55 (s, 1H), 8.14 (s, 1H), 8.67 (t, 1H, J = 5.2 Hz), 8.91 (t, 1H, J = 5.2 Hz); ^{13}C NMR (100 MHz, CDCl$_3$) δ (ppm): 13.7, 13.8, 20.2, 31.1, 31.3, 31.5, 34.3, 39.1, 39.3, 71.1, 72.1, 74.0, 74.5, 122.2, 124.4, 125.7, 125.9, 126.0, 126.9, 127.1, 127.2, 127.3, 127.4, 127.6, 128.7, 129.6, 131.6, 132.3, 133.8, 142.8, 143.5, 148.0, 148.5, 148.9, 149.6, 151.5, 153.2, 167.9, 168.3; IR (KBr, cm^{-1}) ν 3350, 3049, 2959, 2868, 1682, 1537, 1298, 874; MS (m/z): HRMS (ESI) Calcd for C$_{57}$H$_{80}$N$_2$NaO$_7$ ([M+Na]$^+$): 927.5858, found: 927.5874.

7,13,19,25-tetra-*tert*-butyl-28,30-di-hydroxy-27,29-di-(N-pentyl-aminocarbonylmethoxyl)-2,3-dihomo-3-oxacalix[4]arene (4L): Light yellow solid, m.p. 117.7–119.3°C, yield: 72.4% (**Figure S14**); ^{1}H NMR (400 MHz, CDCl$_3$) δ (ppm): 0.67 (t, 3H, J = 7.2 Hz), 0.82 (t, 3H, J = 7.2 Hz), 1.16, 1.24, 1.26 (4s, 36H), 1.29–1.42 (m, 7H), 1.53–1.67 (m, 5H), 3.15–3.25 (m, 2H), 3.43 (t, 2H, J = 14.0 Hz), 3.50–3.65 (m, 3H), 4.09 (d, 1H, J = 13.6 Hz), 4.17–4.24 (m, 2H), 4.37 (d, 2H, J = 14.4 Hz), 4.41 (d, 1H, J = 10.4 Hz), 4.47 (d, 1H, J = 14.8 Hz), 4.61 (d, 1H, J = 10.0 Hz), 4.73–4.81 (m, 2H), 4.93 (d, 1H, J = 10.4 Hz), 6.87 (d, 1H, J = 2.0 Hz), 7.02 (dd, 2H, J_1 = 11.2 Hz, J_2 = 2.4 Hz), 7.15 (dd, 2H, J_1 = 9.6 Hz, J_2 = 2.0 Hz), 7.22 (q, 2H, J = 2.4 Hz), 7.46 (d, 1H, J = 2.4 Hz), 7.54 (s, 1H), 8.19 (s, 1H), 8.68 (s, 1H), 8.95 (s, 1H); ^{13}C NMR (100 MHz, CDCl$_3$) δ (ppm): 13.8, 14.0, 22.4, 22.5, 29.3, 31.1, 31.3, 31.5, 33.9, 39.4, 39.6, 71.2, 72.1, 73.9, 74.5, 122.2, 124.4, 125.6, 126.0, 126.9, 127.0, 127.2, 127.3, 127.4, 127.7, 128.7, 129.6, 131.6, 132.3, 133.8, 142.9, 143.5, 147.9, 148.5, 148.9, 149.5, 151.5, 152.2, 167.8, 168.3; IR (KBr, cm^{-1}) ν 3348, 3049, 2959, 2868, 1682, 1599, 1537, 1485, 1445, 874; MS (m/z): HRMS (ESI) Calcd for C$_{59}$H$_{84}$N$_2$NaO$_7$ ([M+Na]$^+$): 955.6176, found: 955.6174.

7,13,19,25-tetra-*tert*-butyl-28,30-di-hydroxy-27,29-di-(N-clopentyl-aminocarbonylmethoxyl)-2,3-dihomo-3-oxacalix[4]arene (4M): White solid, m.p. 145.9–148.2°C, yield: 83.61% (**Figure S15**); ^{1}H NMR (400 MHz, DMSO-d_6) δ (ppm): 1.12, 1.22, 1.25, 1.26 (4s, 36H), 1.51–1.72 (m, 12H), 1.87–1.96 (m, 4H), 3.49 (q, 2H, J = 6.4 Hz), 3.58 (d, 1H, J = 13.2 Hz), 4.19–4.26 (m, 5H), 4.34–4.42 (m, 3H), 4.47 (d, 1H, J = 14.8 Hz), 4.57 (d, 1H, J = 14.8 Hz), 4.65–4.72 (m, 2H), 4.93 (d, 1H, J = 10.0 Hz), 6.95, 7.05, 7.10 (3s, 3H), 7.29 (d, 2H, J = 8.4 Hz), 7.35 (s, 1H), 7.46 (s, 1H), 7.60 (s, 2H), 8.14 (s, 1H), 8.32 (d, 1H, J = 7.6 Hz), 8.47 (d, 1H, J = 7.2 Hz); ^{13}C NMR (100 MHz, DMSO-d_6) δ (ppm): 24.1, 31.3, 31.5, 31.8, 32.4, 32.8, 33.0, 34.1, 34.4, 50.7, 50.8, 71.5, 74.1, 74.5, 122.3, 124.1, 126.0, 126.1, 126.3, 127.1, 127.3, 128.2, 129.4, 132.3, 132.9, 134.1, 142.1, 142.5, 147.2, 147.4, 149.5, 151.8, 153.9, 167.6, 168.1; IR (KBr, cm^{-1}) ν 3342, 3049, 2961, 2870, 1682, 1529, 1483; MS (m/z): HRMS (ESI) Calcd for C$_{59}$H$_{80}$N$_2$NaO$_7$ ([M+Na]$^+$): 951.5858, found: 951.5862.

7,13,19,25-tetra-*tert*-butyl-28,30-di-hydroxy-27,29-di-(N-benzyl-aminocarbonylmethoxyl)-2,3-dihomo-3-oxacalix[4]arene (4N): m.p. 183.7–186.4°C, yield: 72.0% (**Figure S16**); ^{1}H NMR (400 MHz, CDCl$_3$) δ (ppm): 1.12, 1.20, 1.25 (4s, 36H), 3.32 (t, 2H, J = 12.8 Hz), 3.42 (d, 1H, J = 13.6 Hz), 3.90 (d, 1H, J = 13.6 Hz), 4.03 (dd, 2H, J_1 = 13.2 Hz, J_2 = 4.4 Hz), 4.15 (dd, 2H, J_1 = 15.6 Hz, J_2 = 10.0 Hz), 4.26–4.32 (m, 2H), 4.41–4.57 (m, 4H), 4.64 (s, 1H), 4.67 (d, 1H, J = 4.0 Hz), 4.74 (dd, 1H, J_1 = 14.4 Hz, J_2 = 6.4 Hz), 4.83 (dd, 1H, J_1 = 14.4 Hz, J_2 = 6.4 Hz), 6.79 (d, 1H, J = 2.4 Hz), 6.92 (d, 1H, J = 2.4 Hz), 6.98 (d, 1H, J =

2.8 Hz), 7.04–7.11 (m, 6H), 7.13 (s, 1H), 7.15 (d, 1H, J = 2.4 Hz), 7.19–7.24 (m, 3H), 7.27 (d, 1H, J = 1.6 Hz), 7.28 (s, 1H), 7.38 (dd, 3H, J_1 = 5.8 Hz, J_2 = 2.0 Hz), 7.74 (s, 1H), 8.93 (t, 1H, J = 5.6 Hz), 9.25 (t, 1H, J = 5.6 Hz); ^{13}C NMR (100 MHz, CDCl$_3$) δ (ppm): 31.1, 31.2, 31.5, 31.6, 33.9, 34.2, 43.6, 43.8, 72.2, 73.8, 122.3, 124.5, 125.5, 125.7, 126.1, 126.6, 126.7, 126.9, 127.0, 127.2, 127.3, 127.5, 128.4, 128.5, 128.7, 129.4, 131.4, 132.1, 133.7, 137.4, 138.0, 142.6, 143.2, 148.0, 148.3, 148.7, 149.6, 151.3, 153.0, 168.1, 168.5; IR (KBr, cm^{-1}) ν 3448, 3389, 2955, 2870, 1670, 1485, 1439; MS (m/z): HRMS (ESI) Calcd for C$_{63}$H$_{77}$N$_2$O$_7$ ([M+H]$^+$): 973.5725, found: 973.5716.

7,13,19,25-tetra-*tert*-butyl-28,30-di-hydroxy-27,29-di-(N-phenethyl-aminocarbonylmethoxyl)-2,3-dihomo-3-oxacalix [4]arene (4O): White solid, m.p. 114.6–115.9°C, yield: 67.1% (**Figure S17**); ^{1}H NMR (400 MHz, CDCl$_3$) δ (ppm): 1.15, 1.24, 1.27, 1.28 (4s, 36H), 2.88–3.04 (m, 4H), 3.27 (d, 1H, J = 13.2 Hz), 3.32 (d, 1H, J = 12.8 Hz), 3.46–3.58 (m, 3H), 3.84–3.98 (m, 4H), 4.14 (d, 1H, J = 13.2 Hz), 4.18 (d, 1H, J = 10.4 Hz), 4.32 (d, 1H, J = 10.0 Hz), 4.37 (d, 1H, J = 14.8 Hz), 4.43 (d, 1H, J = 8.8 Hz), 4.46 (d, 1H, J = 3.6 Hz), 4.73 (d, 1H, J = 7.6 Hz), 4.76 (d, 1H, J = 8.0 Hz), 4.88 (d, 1H, J = 10.4 Hz), 6.85 (d, 1H, J = 1.6 Hz), 6.94–6.99 (m, 2H), 7.03–7.22 (m, 14H), 7.43 (d, 1H, J = 2.0 Hz), 7.48 (s, 1H), 8.05 (s, 1H), 8.79 (t, 1H, J = 5.2 Hz), 9.01 (t, 1H, J = 5.6 Hz); ^{13}C NMR (100 MHz, CDCl$_3$) δ (ppm): 31.1, 31.3, 31.6, 32.4, 33.9, 34.2, 35.1, 35.5, 40.6, 40.6, 71.1, 72.0, 73.9, 74.4, 122.2, 124.2, 125.5, 125.9, 126.0, 126.1, 126.2, 126.8, 127.0, 127.2, 127.5, 127.7, 128.2, 128.4, 128.5, 128.7, 129.6, 131.6, 132.4, 133.8, 138.6, 138.9, 142.8, 143.5, 147.9, 148.5, 148.8, 149.3, 151.4, 153.0, 168.0, 168.5; IR (KBr, cm^{-1}) ν 3346, 2961, 2905, 2866, 1682, 1537, 1483, 1445, 1364; MS (m/z): HRMS (ESI) Calcd for C$_{65}$H$_{80}$N$_2$NaO$_7$ ([M+Na]$^+$): 1023.5860, found: 1023.5870.

7,13,19,25-tetra-*tert*-butyl-28,30-di-hydroxy-27,29-di-(N-(3,4-dimethoxyphenethyl)-aminocarbonylmethoxyl)-2,3-dihomo-3-oxacalix [4]arene (4P): White solid, m.p. 117.4–120.1°C, yield: 76.4% (**Figure S18**); ^{1}H NMR (400 MHz, CDCl$_3$) δ (ppm): 1.14, 1.23, 1.24, 1.25 (4s, 36H), 2.86–2.95 (m, 4H), 3.34 (d, 2H, J = 12.0 Hz), 3.46 (d, 1H, J = 13.6 Hz), 3.50–3.60 (m, 2H), 3.72–3.82 (m, 12H), 3.90–4.07 (m, 5H), 4.15 (d, 1H, J = 10.4 Hz), 4.28 (d, 1H, J = 9.2 Hz), 4.35–4.46 (m, 3H), 4.68 (t, 2H, J = 14.4 Hz), 4.81 (d, 1H, J = 10.0 Hz), 6.49 (d, 1H, J = 8.0 Hz), 6.58 (d, 1H, J = 7.2 Hz), 6.64 (d, 1H, J = 7.6 Hz), 6.73 (s, 3H), 6,84 (s, 1H), 7.00 (d, 2H, J = 12.8 Hz), 7.15 (t, 4H, J = 17.6 Hz), 7.41 (s, 1H), 7.51 (s, 1H), 7.94 (s, 1H), 8.76 (s, 1H), 8.90 (s, 1H); ^{13}C NMR (100 MHz, CDCl$_3$) δ (ppm): 30.9, 31.1, 31.2, 31.5, 33.9, 34.2, 34.3, 34.8, 35.1, 40.7, 55.8, 55.9, 70.9, 71.8, 73.9, 111.2, 111.3, 111.8, 112.0, 120.6, 120.7, 122.3, 127.1, 127.2, 127.4, 128.6, 131.3, 131.6, 133.8, 142.8, 143.3, 147.4, 148.0, 148.6, 148.9, 149.1, 151.4, 152.8, 168.0, 168.5; IR (KBr, cm^{-1}) ν 3348, 3049, 2957, 2868, 1682, 1516, 1485, 1362, 874.

7,13,19,25-tetra-*tert*-butyl-28,30-di-hydroxy-27-(N-clopentyl-aminocarbonylmethoxyl)-29-(N-(2-hydroxyethyl)-aminocarbonylmethoxyl)-2,3-dihomo-3-oxacalix[4]arene (4Q): White solid, yield: 82.5%, m.p. 138.3–140.5°C (**Figure S19**); ^{1}H NMR (400 MHz, CDCl$_3$) δ (ppm): 1.14, 1.19, 1.24, 1.26 (4s, 36H), 1.59–1.80 (m, 8H), 3.32–3.52 (m, 4H), 3.56 (d, 1H, J = 13.8 Hz), 3.67–3.79 (m, 4H), 4.05–4.22 (m. 4H),

4.31–4.45 (m, 5H), 4.52–4.60 (m, 2H), 4.69–4.91 (m, 3H), 4.99 (d, 1H, J = 10.8 Hz), 6.86–7.13 (m, 6H), 7.22 (d, 2H, J = 8.0 Hz), 7.37 (d, 1H, J = 5.6 Hz), 7.86 (d, 1H, J = 14.0 Hz), 8.70–9.01 (m, 2H); ^{13}C NMR (100 MHz, CDCl$_3$) δ (ppm): 23.9, 24.1, 31.0, 31.2, 31.4, 31.6, 32.0, 32.4, 32.9, 33.3, 33.9, 42.6, 51.2, 62.0, 71.5, 72.0, 122.3, 124.2, 125.5, 125.8, 126.1, 126.9, 127.1, 127.3, 127.5, 127.7, 128.4, 129.4, 131.7, 132.2, 133.6, 143.0, 143.5, 147.7, 148.0, 148.5, 148.9, 149.6, 150.0, 151.3, 153.6, 168.8, 169.0; IR (KBr, cm^{-1}) ν 3350, 2961, 2870, 1674, 1485, 1298, 1196, 1070; MS (m/z): HRMS (ESI) Calcd for C$_{56}$H$_{76}$N$_2$NaO$_8$ ([M+Na]$^+$): 927.5499, found: 927.5486.

7,13,19,25-tetra-tert-butyl-28,30-di-hydroxy-27-(N-phenethyl-aminocarbonylmethoxyl)-29-(N-(2-hydroxyethyl)-aminocarbonylmethoxyl)-2,3-dihomo-3-oxacalix[4]arene (4R): White solid, m.p. 120.7–123.3°C, yield: 81.6% (**Figure S20**); ^{1}H NMR (400 MHz, CDCl$_3$) δ (ppm): 1.00 (s, 3H), 1.14 (s, 6H), 1.18 (s, 6H), 1.21 (s, 3H), 1.24 (s, 6H), 1.26 (s, 9H), 1.28 (s, 3H), 2.87–3.04 (m, 3H), 3.26–3.38 (m, 1H), 3.42–3.53 (m, 3H), 3.54–3.64 (m, 2H), 3.70–3.78 (m, 2H), 4.00–4.11 (m, 2H), 4.23 (dd, 2H, J_1 = 12.0 Hz, J_2 = 7.8 Hz), 4.30 (d, 1H, J = 10.4 Hz), 4.38–4.43 (m, 2H), 4.50 (dd, 2H, J_1 = 14.8 Hz, J_2 = 9.6 Hz), 4.61 (dd, 1H, J = 16.4, 6.6 Hz), 4.71 (dd, 1H, J_1 = 15.4 Hz, J_2 = 5.8 Hz), 4.83 (dd, 1H, J_1 = 10.2 Hz, J_2 = 5.6 Hz), 6.79–6.89 (m, 1H), 6.94–7.03 (m, 3H), 7.03–7.11 (m, 2H), 7.11–7.15 (m, 3H), 7.16 (d, 3H, J = 4.4 Hz), 7.22 (s, 1H), 7.34–7.41 (m, 2H), 7.94 (s, 1H), 8.69–8.80 (m, 1H), 8.90 (t, 1H, J = 5.6 Hz); ^{13}C NMR (100 MHz, CDCl$_3$) δ (ppm): 30.9, 31.1, 31.2, 31.5, 31.6, 32.2, 33.9, 34.2, 35.3, 35.5, 40.6, 40.7, 42.5, 62.0, 62.4, 70.9, 71.8, 73.9, 74.3, 122.3, 124.5, 125.6, 125.9, 126.1, 126.2, 126.6, 127.2, 127.3, 127.7, 128.3, 128.4, 128.5, 128.6, 128.7, 129.4, 131.6, 132.2, 133.5, 133.9, 138.7, 138.8, 143.0, 143.6, 148.0, 148.5, 148.7, 148.8, 149.4, 151.3, 152.7, 168.7, 168.9, 169.3; IR (KBr, cm^{-1}) ν 3366, 2961, 2868, 1670, 1541, 1485, 1200, 1072, 874, 579; MS (m/z): HRMS (ESI) Calcd for C$_{59}$H$_{76}$N$_2$NaO$_8$ ([M+Na]$^+$): 963.5494, found: 963.5491.

7,13,19,25-tetra-tert-butyl-28,30-di-hydroxy-27-(N,N-bis(2-hydroxyethyl)-aminocarbonylmethoxyl)-29-(N-(2-hydroxyethyl)-aminocarbonylmethoxyl)-2,3-dihomo-3-oxacalix[4]arene (4S): White solid, m.p. 144.4–146.2°C, yield: 85.9% (**Figure S21**); ^{1}H NMR (400 MHz, CDCl$_3$) δ (ppm): 1.07, 1.23, 1.25, 1.26 (4s, 36H), 3.31–3.58 (m, 8H), 3.68–3.89 (m, 8H), 4.00 (s, 2H), 4.22 (d, 1H, J = 13.2 Hz), 4.36 (d, 1H, J = 13.2 Hz), 4.58 (d, 1H, J = 14.8 Hz), 4.91–5.02 (m, 4H), 6.81 (s, 1H), 6.89 (s, 1H), 7.02 (s, 2H), 7.10 (s, 1H), 7.16 (d, 2H, J = 6.8 Hz), 7.43 (s, 1H), 7.83 (s, 1H), 8.99 (s, 1H), ^{13}C NMR (100 MHz, CDCl$_3$) δ (ppm): 30.6, 31.0, 31.1, 31.6, 31.7, 33.9, 34.1, 34.3, 42.4, 49.9, 51.3, 59.9, 60.0, 62.0, 71.2, 72.2, 72.7, 74.0, 122.8, 124.2, 125.1, 125.5, 15.8, 125.9, 126.6, 128.2, 129.0, 129.2, 129.4, 132.0, 132.2, 134.4, 142.4, 143.0, 146.8, 148.0, 148.9, 150.9, 151.7, 153.7, 170.3, 170.4; IR (KBr, cm^{-1}) ν 3398, 2961, 2870, 1485, 1364, 1202, 1068, 874; MS (m/z): HRMS (ESI) Calcd for C$_{55}$H$_{76}$N$_2$NaO$_{10}$ ([M+Na]$^+$): 947.5398, found: 947.5408.

Crystallography

The single crystal of dihomooxacalix[4]arene amide 4L and 4N were obtained in ethanol and their single crystal structures were determined on a Bruker Smart Apex

single crystal diffractometer. The data were processed with HKL2000. The structure was solved by direct methods of SHELX86 and subsequent Fourier-difference synthesis and refined by full-matrix least-squares on F^2 with SHELXS-97 (Sheldrick, 1997). No absorption correction was done. All non-hydrogen atoms were refined with anisotropic displacement parameters.
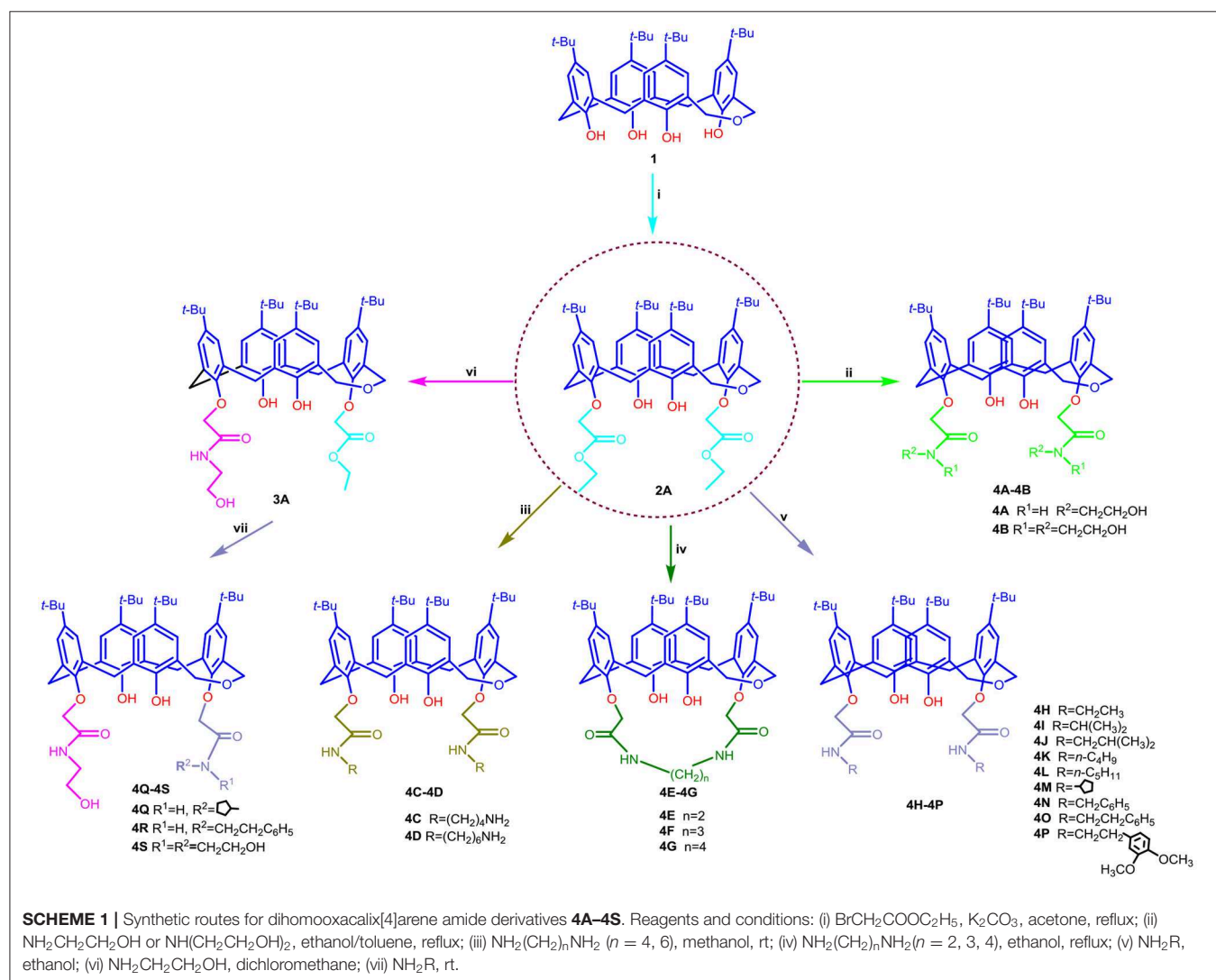
Cell Culture

A549 cells (human lung carcinoma cells), MCF-7 cells (human breast cancer cells), HeLa cells (human cervical cancer cells), HepG2 cells (human hepatocellular carcinoma cells), and HUVEC cells (human umbilical vein endothelial cells) were kindly provided by WeiFang Caleb Pharmaceuticals, Inc. A549 cells were cultured in Ham's F12K medium containing 10% fetal bovine serum, 2 mM L-glutamine, and 1.5 g/L sodium bicarbonate; MCF-7 cells were cultured on cell culture flask using RPMI 1640 medium with 2 mM L-glutamine adjusted to contain 1.5 g/L sodium bicarbonate, 4.5 g/L glucose, 10 mM
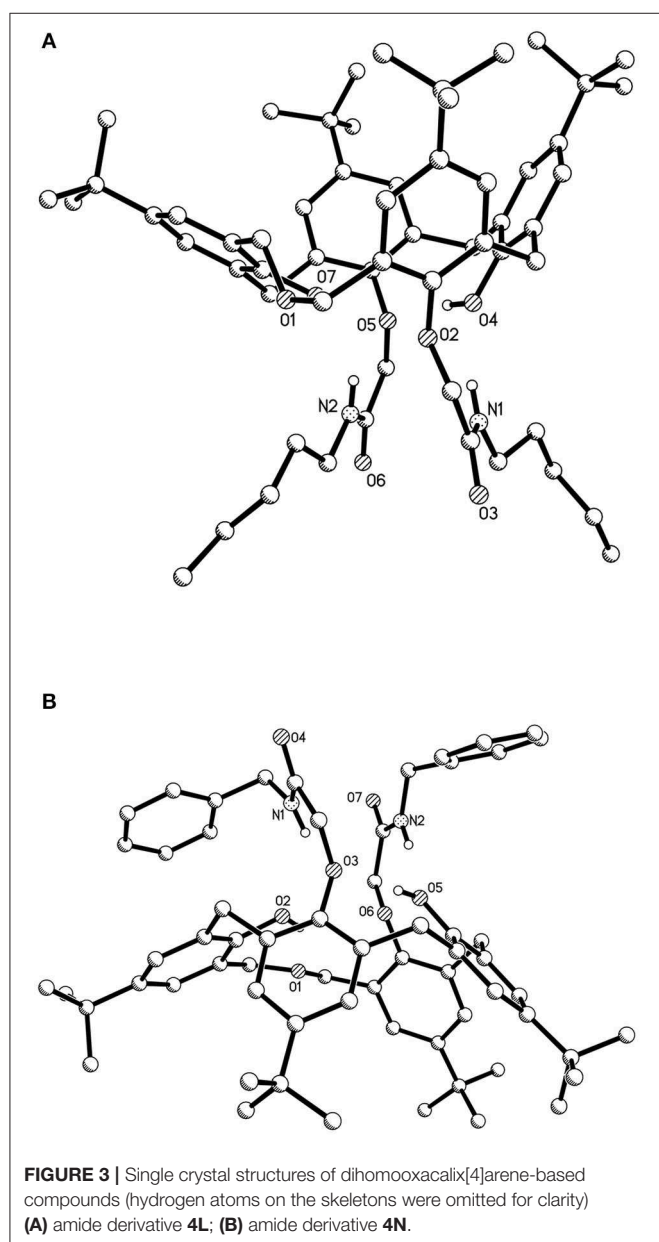
HEPES, 1.0 mM sodium pyruvate, and 10% fetal bovine serum. Hela cells were cultured on Cell culture flask using 2 mM L-glutamine adjusted to contain 1.5 g/L sodium bicarbonate, 4.5 g/L glucose, 10 mM HEPES, and 1.0 mM sodium pyruvate in RPMI 1640 medium supplemented with 0.5 mg/ml G418 and 10% fetal bovine serum. HepG2 cells were cultured in minimum essential medium (Eagle) with 2 mM L-glutamine, Earle's BSS, 1.5 g/L sodium bicarbonate, 0.1 mM non-essential amino acids, 1.0 mM sodium pyruvate, and 10% fetal bovine serum. HUVEC cells were cultured in M199 medium containing 2 mM L-glutamine adjusted to contain 1.5 g/L sodium bicarbonate, 4.5 g/L glucose, 10 mM HEPES, 1.0 mM sodium pyruvate, ECGS, and 10% fetal bovine serum. All cells were cultured at 37°C in 5% CO_2.

Cytotoxicity Assay

The cell proliferation of adherent cells was determined by sulforhodamine B assay (SRB) (Quan et al., 2009; Li et al., 2017). All cells were cultured in culture medium containing 10%

SCHEME 1 | Synthetic routes for dihomooxacalix[4]arene amide derivatives **4A–4S**. Reagents and conditions: (i) $BrCH_2COOC_2H_5$, K_2CO_3, acetone, reflux; (ii) $NH_2CH_2CH_2OH$ or $NH(CH_2CH_2OH)_2$, ethanol/toluene, reflux; (iii) $NH_2(CH_2)_nNH_2$ ($n = 4, 6$), methanol, rt; (iv) $NH_2(CH_2)_nNH_2$ ($n = 2, 3, 4$), ethanol, reflux; (v) NH_2R, ethanol; (vi) $NH_2CH_2CH_2OH$, dichloromethane; (vii) NH_2R, rt.

fetal bovine serum and have been in the logarithmic growth phase. All cell types were seeded in a 96-well culture plate at a concentration of $1–5 \times 10^4$ cells per well at 37°C in a 5% CO_2 incubator for 24 h. The cells were then exposed to seven drug concentrations of dihomooxacalix[4]arene derivatives for 72 h with each concentration located in three wells. Then, the cells were fixed with trichloroacetic acid (TCA). After washing, SRB working solution was added to the cells to clean them. SRB combined with protein was dissolved in Tris base. OD values were measured for each well with a SPECTRA max 190 Cell microplate reader under 540 nm wavelength. According to the OD value, the cell growth inhibition rate was calculated.

FIGURE 3 | Single crystal structures of dihomooxacalix[4]arene-based compounds (hydrogen atoms on the skeletons were omitted for clarity) **(A)** amide derivative **4L**; **(B)** amide derivative **4N**.

Flow Cytometry
Flow Cytometry for Cell Cycle Analysis
For flow cytometric analysis of DNA content, MCF-7 cells in exponential growth were treated with compound for 48 h. The cells treated with compound were collected, washed twice with PBS, and then fixed with 75% alcohol overnight. Then, the cells were washed with PBS and resuspended in 100 µl of PBS, 200 mg/ml RNase was added for 30 min to eliminate the interference of RNA, and 20 ml/L propidium iodide (PI; Sigma) was added for 30 min. Then, the cells were washed, and the DNA content was detected by a flow cytometer (BD Accuri C6).

Flow Cytometry for Cell Apoptosis Analysis
MCF-7 cells (5×10^5 cells/ml) were seeded in six-well plates and treated with compounds at different concentrations for 48 h. The cells were then harvested by trypsinization and washed twice with cold PBS. After centrifugation and removal of the supernatants, cells were resuspended in 400 µl of 1×binding buffer, which was then added to 5 µl of annexin V-FITC and incubated at room temperature for 15 min. After adding 10 µl of PI, the cells were incubated at room temperature for another 15 min in the dark. The stained cells were analyzed by a flow cytometer (BD Accuri C6).
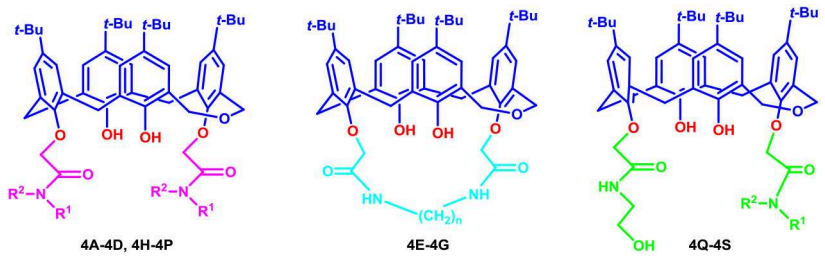
Statistical Analysis
Data were calculated using the non-parametric variance. Comparisons among groups were statistically analyzed. $P < 0.05$ was considered statistically significant. Statistical analyses were conducted using SPSS 16.0 (SPSS, Chicago, IL, USA).
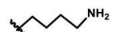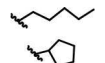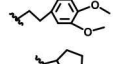
RESULTS AND DISCUSSION
Synthesis Investigation
The routes used for the synthesis of the target compounds **4A—4S** are outlined in **Scheme 1**.

As outlined in **Scheme 1**, all the targets **4A—4S** consist of 1,3-alternate dihomooxacalix[4]arene conformers. As a first step in our development of dihomooxacalix[4] arene amide derivatives, 1,3-di-ethoxycarbonyl substituted dihomooxacalix [4]arene intermediate **2A** initially synthesized as the key intermediate from known *tert*-butyl dihomooxacalix[4]arene **1** by esterification with bromoethyl acetate in the presence of potassium carbonate in refluxing acetone. Subsequently, refluxing ester **2A** with excess ethanolamine or diethanolamine in the mixed ethanol/toluene readily afforded the desired amide derivative **4A—4B** in good yield of 87.2 and 86.7%, respectively. The derivatives **4C—4D** were obtained by reacting ester **2A** with an excess amount of diamines in methanol at low temperature (initially stirring in ice bath, and then up to room temperature) and the satisfying yields was 63.3 to 96.2%. Interestingly, on replacement of methanol with refluxing ethanol, but under otherwise similar conditions, the two amino groups on the diamine were found to react with ester **2A** simultaneously to give amino-bridging products **4E—4G**. To investigate the effect on affinity of different linker groups attached to the amino and dihomooxacalix[4]arene components, compounds **4H—4P** were successfully accomplished by ester

TABLE 1 | Single concentration inhibition of dihomooxacalix[4]arene derivatives **4A–4S** on cell viability.

Compd.	R^1/n	R^2	% inhibition at 10 μM				
			A549	MCF-7	HeLa	HepG2	HUVEC
4A	H	⟍OH	100	100	100	86	41
4B	⟍OH	⟍OH	66	73	100	39	23
4C	H	⟍⟍NH_2	42	78	96	64	55
4D	H	⟍⟍⟍NH_2	99	99	100	72	90
4E	2	–	60	50	46	21	26
4F	3	–	63	46	59	9	42
4G	4	–	21	34	40	16	34
4H	H		31	37	41	31	6
4I	H		45	17	44	9	16
4J	H		54	40	35	10	0
4K	H		65	41	42	6	1
4L	H		66	41	49	18	12
4M	H		66	29	52	12	14
4N	H		64	43	49	10	21
4O	H		63	45	60	9	35
4P	H		22	0	37	11	0
4Q	H		34	0	49	23	18
4R	H		2	0	4	−1	85
4S	⟍OH	⟍OH	89	96	97	94	21
CLX-4	–	–	93	99	92	94	16
Paclitaxel	–	–	$IC_{50} = 0.59$ nM	$IC_{50} = 0.8$ nM	$IC_{50} = 2.7$ nM	$IC_{50} = 5.0$ nM	$IC_{50} = 1.0$ nM

2A with aliphatic primary amine by method similar to that for compounds **4C−4D**. However, secondary amine was not ideal for the same condition in that of steric hindrance. In addition, treatment of **2A** with ethanolamine in dichloromethane resulted in the partial aminolysis, leading to the generation of mono-N-(2-hydroxyethyl)-aminocarbonyl dihomooxacalix[4]arene compound **3A**, which was further reacted with aliphatic primary amine in methanol to yield the amide derivatives **4Q−4S**. Separation of the reaction products into the pure compounds **4A−4S** was achieved by column chromatography. All the synthesized compounds were further characterized by IR, ^{1}H NMR, ^{13}C NMR, and HR-MS spectrometry.

Single Crystal Structure Analysis

The single crystal structures of dihomooxacalix[4]arene amide derivatives **4L** and **4N** are shown in **Figure 3**. The crystal data, data collection, and structure refinements are summarized in **Table S1**.

As shown in **Figure 3A**, the conformation of dihomooxacalix[4]arene derivative **4L** crystallizes in the monoclinic space group of P 21/c. In molecules, the two N-pentyl-aminocarbonylmethoxyl groups (27, 29-positions) at the lower rim of the rings exist in 1,3-distal position. The four phenolic rings remained standing on same side of the mean plane defined by the four phenolic oxygen atoms O2, O4, O5, and O7. One of the aromatic rings, bearing O7, is partly parallel

to the mean plane [dihedral angle: 27.013° (148)]. The remaining three aromatic rings, bearing O2, O4, O5, respectively, are 70.627° (40), 66.852° (38), and 62.138° (42). The 27, 29-di-(N-benzyl-aminocarbonylmethoxyl) dihomooxacalix[4]arene amide derivatives **4N** (**Figure 3B**) possessing the cone conformation shows some interesting similarities with **4L**. It crystallizes the monoclinic space group of C 2/c. The two benzyl groups are located at slightly longer distances but on the same side of the mean plane defined by O2, O3, O5, and O6 atoms. The dihedral angles of the four aromatic rings are 20.904° (71), 78.442° (69), 52.4762° (57), and 54.069° (59).

Compounds 4A−4S Reduce the Viability of Cancer Cells

The cell-based assay can provide a useful tool to screen the preliminary specificity (Zhou et al., 2006). From this point, the synthesized compounds **4A−4S** were evaluated for antitumor activity against A549 cells, MCF-7 cells, HeLa cells, and HepG2 cells, as well as HUVEC cells using the SRB method. For initial screening, the single concentration inhibition of compounds **4A−4S** on cell viability at a concentration of 10 μM was assessed 72 h after treatment in comparison with those of reference compound **CLX-4** and the positive control (paclitaxel). The results are summarized in **Table 1**.

As shown in **Table 1**, dihomooxacalix[4] arene derivative **4A,** which still maintains the original N-(2-hydroxyethyl) aminocarbonyl group of precursor **CLX-4**, is the most effective at inducing cytotoxicity in all the four tumor cell types tested with the single concentration inhibition on the four tumor cells ranging from 86 to 100%. The potency is equivalent to that of **CLX-4**. It allows us to conclude that the replacement of calix[4]arene bone with the dihomooxacalix[4]arene scaffold is successful. Encouraged by it, the modification of 2-hydroxyethyl

group adjacent to the amido unit of the benzene ring is considered. Thus, a range of substituents, such as alkyl groups with straight or branched chains, alkyl benzyl, and alkyl amino substitution are introduced to the R2 position linked on the amido unit to afford 12 amide derivatives, including **4B-4D**, **4H−4P**. It is revealed that the majority of the above 12 amide derivatives demonstrate a good selectivity profile on A549 cell lines, but display the weak anti-tumor effects on hepG2 cell lines. In this series, derivative **4C** has the selective effect on HeLa cells. In a contrast, compound **4D** with much longer alkyl chain exerts the markable inhibition on all the tested tumor cells. In addition, derivatives with hydroxyethyl or alkyl amino group, e.g., **4A−4D** are particularly more effective than those of bearing alkyl unit with low polarity and hydrophilicity (**4H−4K**) or containing alkyl benzyl group with big steric hindrance (**4P**). Therefore, the inhibition efficiency of those derivatives is significantly involved in the hydrophilicity, steric hindrance, hydrogen bonding, and polarity of the R2 functional groups.

Moreover, the toxicity of those derivatives on HUVEC cells was also investigated. The result indicates that within a reasonable range, the single concentration inhibition of **4A** is 41%, though slightly higher than 18% of **CLX-4.** However, either **4C** or **4D** has much toxicity on HUVEC cell lines with inhibition of 55 and 90%, respectively. This may be due to the influence of the bare primary amino group on the side of alkyl chain. In this way, the further structural optimization was carried and the bridged derivatives **4E−4G** were afforded. As we expected, the toxicity of **4E−4G** on HUVEC cell lines is decreased with the single concentration inhibition degree varying from 16 to 42%. Meanwhile their inhibitory activity is less potent than those of **4C** and **4D**. Thus, N-2-hydroxyethyl attached to amido unit is probably vital to the activity of those compounds. To verify our assumption, one of the N-2-hydroxyethyl groups is replaced by cyclopentyl, phenethyl, or N,N-di-2-hydroxyethyl substituent to give **4Q−4S**.

In this series, compound **4Q** indicated no effect on MCF-7 cell line and indicated about two - to threefold decrease in potency of three other tumor cell lines, compared with those of **CLX-4**. Compound **4R** exerted no viability on the tested tumor cells, but had serious toxicity on HUVEC cell lines. As a contrast, compound **4S** remains a similar antitumor level activity to **CLX-4**, which is essentially in agreement with that of **4A**. The absence of significant activity in **4Q** and **4R** proved that N-2-hydroxyethyl substituent linked on the amido unit is suggested to have a significant impact on the inhibition activity.
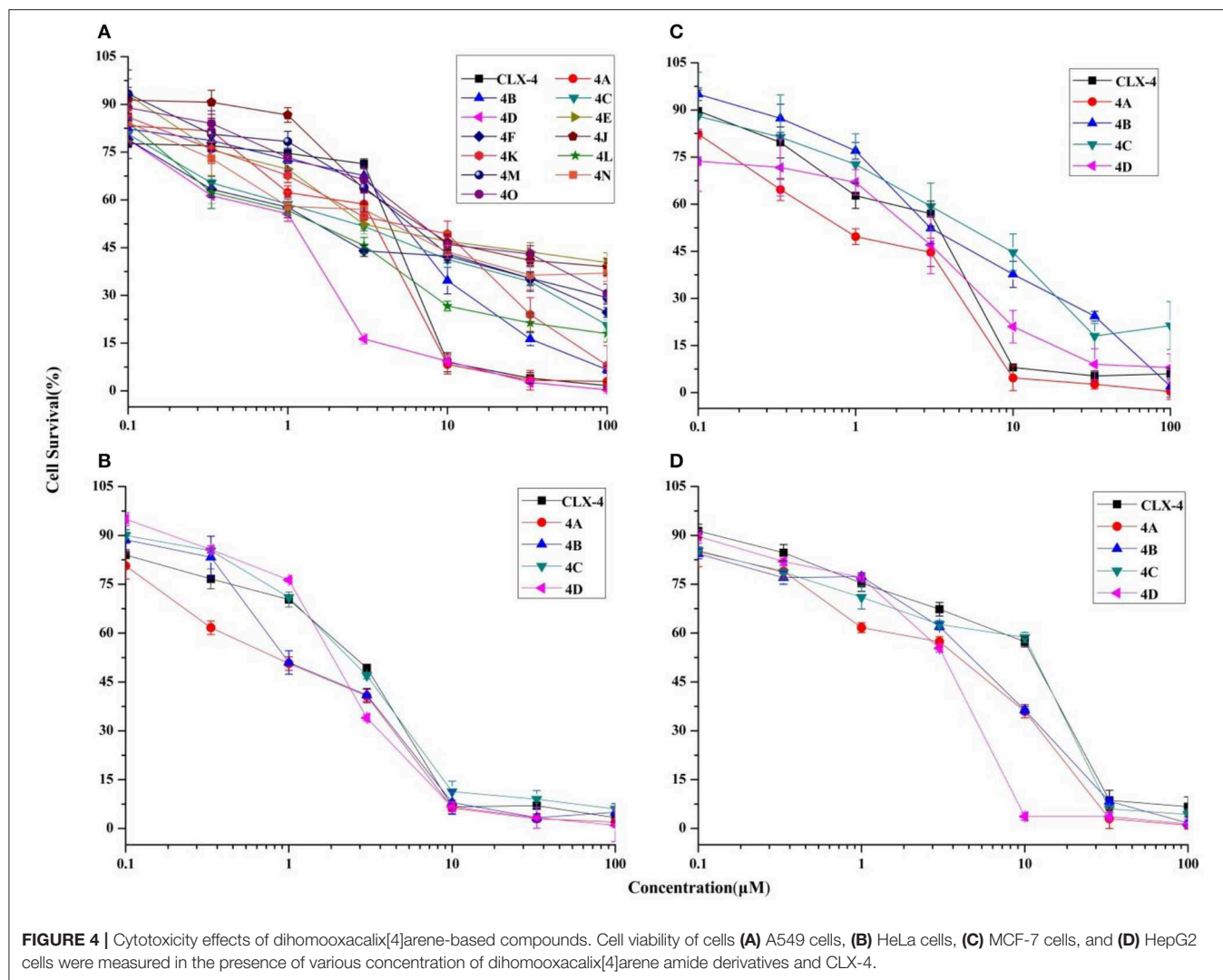
Based on the results of initial screening, the determined IC_{50} values of potent dihomooxacalix[4]arene amides for tumor cell viability are measured and described in **Table 2**. Dose–response curves are shown in **Figure 4**.

Our data in **Table 2** shows that almost all dihomooxacalix[4]arene amides exert satisfying potency on A549 cell lines. Compounds **4A−4D** exerted potent growth inhibition against various human cancer cells with IC_{50} values ranging narrowly from 0.6 to 8.0 μM. In particular, **4A** demonstrates the greatest cytotoxic effect against cervical cancer (HeLa) cell line with the IC_{50} of 0.8 ± 0.2 μM, which is at the

TABLE 2 | IC_{50} values of dihomooxacalix[4]arene-based compounds on tumor cells viability.

Compd.	IC_{50} (μM)			
	A549	MCF-7	HeLa	HepG2
4A	2.0 ± 0.5	1.0 ± 0.1	0.8 ± 0.2	2.7 ± 0.4
4B	3.9 ± 0.5	4.4 ± 0.7	1.1 ±0.5	3.8 ± 0.3
4C	3.3 ± 0.7	5.4 ± 2.6	2.3 ± 0.1	5.0 ± 0.8
4D	0.7 ± 0.1	1.8 ± 0.7	1.9 ± 0.1	2.6 ± 0.2
4E	12.4 ± 2.2	–	–	–
4F	2.9 ± 0.7	–	–	–
4J	16.9 ± 3.2	–	–	–
4K	4.5 ± 1.4	–	–	–
4L	1.7 ± 0.4	–	–	–
4M	10.1 ± 1.8	–	–	–
4N	6.8 ± 0.5	–	–	–
4O	12.6 ± 2.0	–	–	–
CLX-4	2.8 ± 0.3	2.1 ± 0.4	1.9 ± 0.2	6.6 ± 0.8

"N.T." means no tested.

FIGURE 4 | Cytotoxicity effects of dihomooxacalix[4]arene-based compounds. Cell viability of cells **(A)** A549 cells, **(B)** HeLa cells, **(C)** MCF-7 cells, and **(D)** HepG2 cells were measured in the presence of various concentration of dihomooxacalix[4]arene amide derivatives and CLX-4.

level of submicromolar concentration. Overall, **4A** and **4D** show enhanced potency over the cytotoxicity profiles (2- to 4-fold) of **CLX-4**, suggesting that our structural optimization is successful.

Flow Cytometry for MCF-7 Cell Cycle and Apoptosis Analysis

Cancer progression has been suggested to include the loss of cell cycle checkpoint controls that regulate passage through the cell cycle (Pelizzarorocha et al., 2013; Ji et al., 2017). According to the literatures, Dings and co-workers (Dings et al., 2013) have revealed that calixarene amine derivative **PTX013** had good cytotoxicity to cancer cells and blockades the cell cycle of SQ20B at G0/G1 phase. In addition, Pelizzarorocha et al. (2013) found that *tert*-butyl calix[6]arenes can cause cell cycle arrest in G0/G1 phase by down-regulating key proteins, such as PIM1, CDK2, and CDK4. To have an insight into the underlying mechanism of cytotoxic effects *in vitro*, the key indicators including the cell cycle and apoptosis were observed by the flow cytometry analysis. We first tested if treatment with **4A** or **4D** affects the cell cycle of MCF-7 cells. The results are shown in **Figure 5**.

As exemplified with MCF-7 cells in **Figure 5A**, the percentage of non-treated cells was 61.36 ± 3.65% in G0/G1 phase, 24.69 ± 6.30% in S, and 10.06 ± 0.91 in G2/M phase, whereas after the treatment with **4A** at a low concentration (3 μM) for 48 h, MCF-7 cells led to an accumulation number of cells in G0/G1 phase of the cell cycle and the percentage was increased to 71.39 ± 11.21%, whereas it correspondingly reduced to 20.68 ± 13.12% and 1.87 ± 2.45%, respectively, in S and G2/M phase. A similar profile in the cells treated with 3 μM **4D** was supported by the 73.56 ± 3.95% of cells in the G0/G1 phase, as observed in **Figure 5B**.

Next, we measured the apoptotic rate of MCF-7 cells at different concentrations of treatment to detect whether 4A and 4D can induce apoptosis. As shown in **Figure 6**, during treatment of MCF-7 cells for 48 h with 1 and 3 μM of 4A, 19.63 ± 0.11% and 15.40 ± 0.13% apoptotic rates are given by the contrast of 14.50 ± 0.68% in the non-treated group, which suggests that 1 or 3 μM of 4A is not enough to induce apoptosis in MCF-7 cells. Subsequently, treatment of MCF-7 cells with 10 μM of 4A resulted in the progressive apoptotic
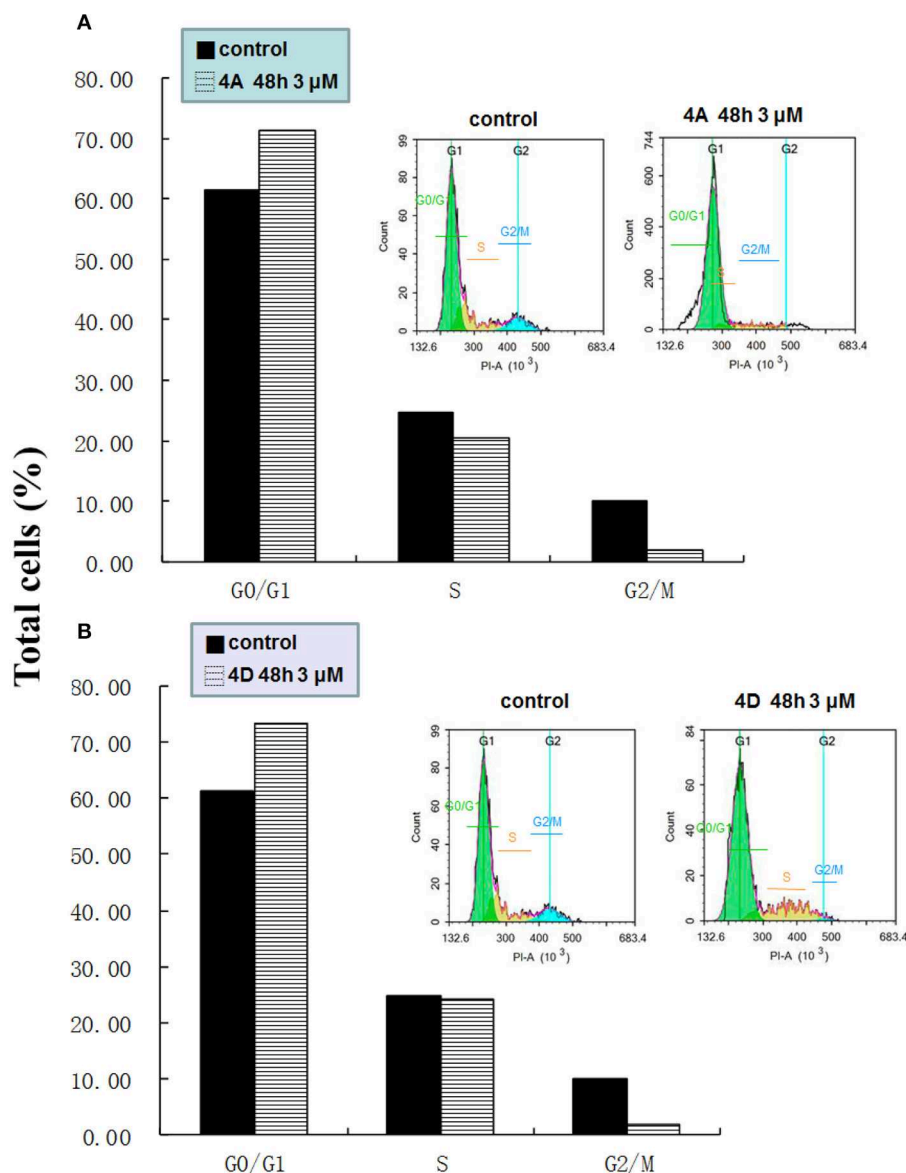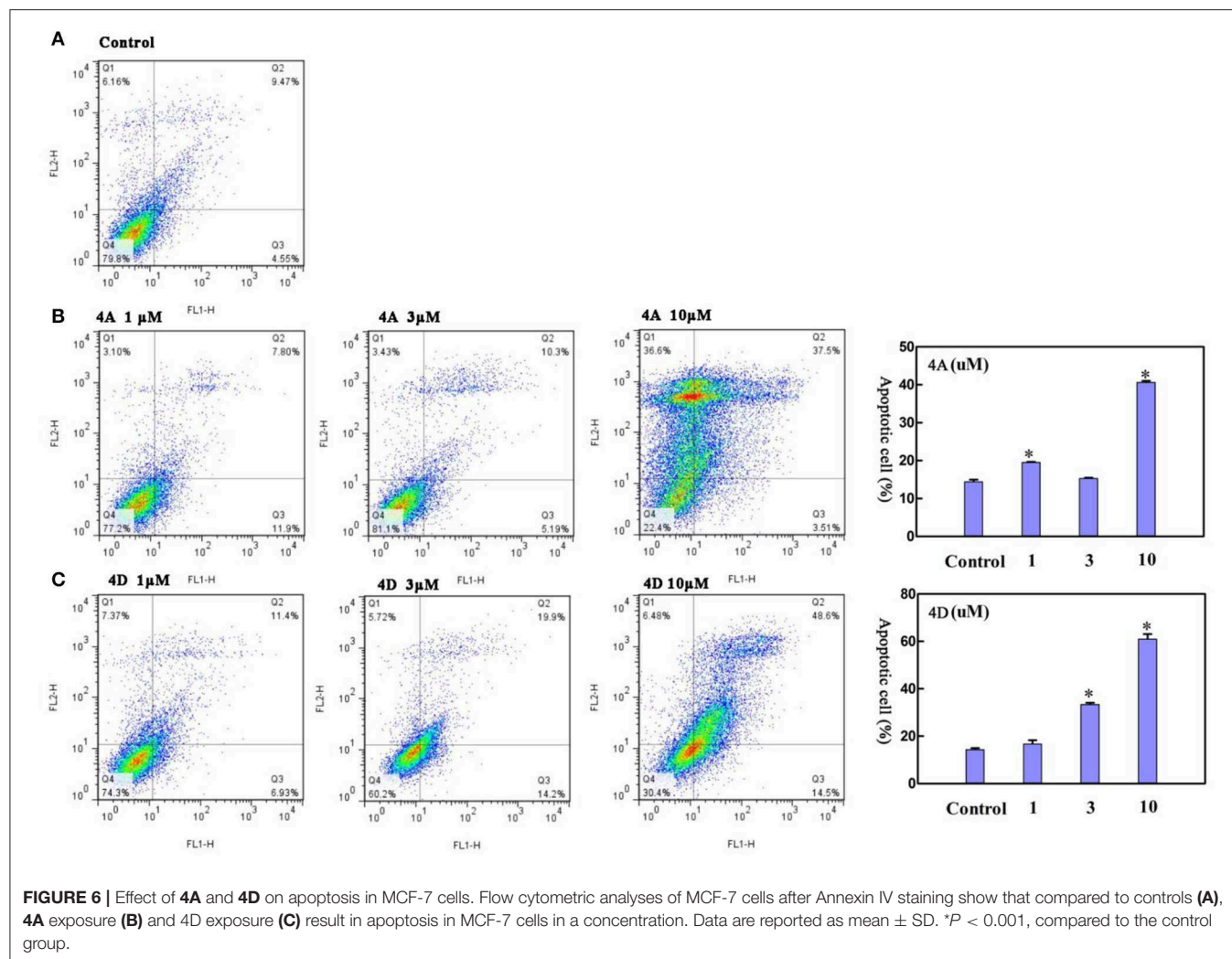
FIGURE 5 | Effect of **4A** and **4D** on the cell cycle of MCF-7 cells. Flow cytometric analyses of MCF-7 cells show that **4A (A)**, **4D (B)** treatment induces G0/G1 arrest in MCF-7.

rate of $40.74 \pm 0.38\%$. This proliferation is also observed after the treatment of 4D at concentrations of 3 and $10\,\mu M$, supported by apoptotic rates of $33.55 \pm 0.78\%$ and $61.15 \pm 2.76\%$ (**Figure 6C**). Therefore, we conclude that both 4A and 4D can induce cell apoptosis in MCF-7 cells as well as cell cycle arrest in G0/G1 phase.

CONCLUSION

In summary, this study describes the optimization of the anti-tumor agent CLX-4 by employing the drug design strategies, X-ray crystallography, and cell-based screening. With the comparison to CLX-4, dihomooxacalix[4]arene derivative 4A demonstrates the much more efficient cytotoxic effect against the MCF-7 and HeLa cell lines with IC_{50} of $1.0 \pm 0.1\,\mu M$ and $0.8 \pm 0.2\,\mu M$, respectively. Derivative 4D has an IC_{50} of $0.7 \pm 0.1\,\mu M$ against A549 cell lines, but failed due to the high toxicity on HUVEC cell lines. The underlying mechanism of cytotoxic effects indicates that they can induce the MCF-7 cell cycle arrest in G0/G1 phase and cell apoptosis. In this context, it is also important to note that we provide a new look into drug discovery by using the old supramolecuar scaffold to design potent anti-tumor agents.

FIGURE 6 | Effect of **4A** and **4D** on apoptosis in MCF-7 cells. Flow cytometric analyses of MCF-7 cells after Annexin IV staining show that compared to controls **(A)**, **4A** exposure **(B)** and 4D exposure **(C)** result in apoptosis in MCF-7 cells in a concentration. Data are reported as mean ± SD. *$P < 0.001$, compared to the control group.

DATA AVAILABILITY STATEMENT

The detailed spectroscopic data including crystallographic data (CIF) of compounds are available. Single crystal data for compounds **4L** and **4N** have been deposited in the Cambridge Crystallographic Data Center and assigned to deposition numbers CCDC 1915578 and 1569156. All datasets generated for this study are included in the article/**Supplementary Material**.

AUTHOR CONTRIBUTIONS

LA and CY designed the work. LH, CW, and JL made contributions to the experiments and collective data. The paper was written by LA. YZ, TH, and JS provide the technical support. All authors extensively discussed the results, reviewed the manuscript, extensively discussed the results, reviewed the manuscript, and approved the final version of the manuscript to be submitted.

FUNDING

SUPPLEMENTARY MATERIAL

The Supplementary Material for this article can be found online at: https://www.frontiersin.org/articles/10.3389/fchem.2019.00856/full#supplementary-material

REFERENCES

Ali, Y., Muhamad Bunnori, N., Susanti, D., Muhammad Alhassan, A., and Abd Hamid, S. (2018). Synthesis, *in-vitro* and *in silico* studies of azo-based calix[4]arenes as antibacterial agent and neuraminidase inhibitor: a new look into an old scaffold. *Front. Chem.* 6, 210–219. doi: 10.3389/fchem.2018.00210

An, L., Han, L. L., Zheng, Y. G., Peng, X. N., Xue, Y. S., Gu, X. K., et al. (2016). Synthesis, x-ray crystal structure and anti-tumor activity of calix[n]arene polyhydroxyamine derivatives. *Eur.J. Med. Chem.* 123, 21–30. doi: 10.1016/j.ejmech.2016.07.016

An, L., Wang, J. W., Wang, C., Zhou, S. S., Sun, J., and Yan, C. G. (2018). 2, 3-Ethylene-bridged dihomooxacalix [4] arenes: synthesis, X-ray crystal structures and highly selective binding properties with anions. *New J. Chem.* 42, 10689–10696. doi: 10.1039/C8NJ01284A

Bauer, D., Andrae, B., Gaß, P., Trenz, D., Becker, S., and Kubik, S. (2019). Functionalisable acyclic cucurbiturils. *Org. Chem. Front.* 6, 1555–1560. doi: 10.1039/C9QO00156E

Böhmer, V. (2010). Calixarenes, macrocycles with (almost) unlimited possibilities. *Angew. Chem, Int. Ed. Engl.* 34, 713–745. doi: 10.1002/anie.199507131

Chen, J., Wang, Y., Wang, C., Long, R., Chen, T., and Yao, Y. (2019). Functionalization of inorganic nanomaterials with pillar [n] arenes. *Chem. Comm.* 55, 6817–6826. doi: 10.1039/C9CC03165K

Consoli, G. M., Cunsolo, F., Geraci, C., and Sgarlata, V. (2004). Synthesis and lectin binding ability of glycosamino acid–calixarenes exposing GlcNAc clusters. *Org. Lett.* 6, 4163–4166. doi: 10.1021/ol0485767

Consoli, G. M. L., Granata, G., Picciotto, R., Blanco, A. R., Geraci, C., Marino, A., et al. (2018). Design, synthesis and antibacterial evaluation of a polycationic calix[4]arene derivative alone and in combination with antibiotics. *Med. Chem. Commun.* 9, 160–164. doi: 10.1039/C7MD00527J

Da Silva, E., Lazar, A. N., and Coleman, A. W. (2004). Biopharmaceutical applications of calixarenes. *J. Drug. Deliv. Sci. TEC.* 14, 3–20. doi: 10.1016/S1773-2247(04)50001-1

Dings, R. P., Levine, J. I., Brown, S. G., Astorguesxerri, L., Macdonald, J. R., Hoye, T. R., et al. (2013). Polycationic calixarene ptx013, a potent cytotoxic agent againsttumors and drug resistant cancer. *Invest. New Drugs* 31, 1142–1150. doi: 10.1007/s10637-013-9932-0

Dings, R. P., Miller, M. C., Nesmelova, I., Astorguesxerri, L., Kumar, N., Serova, M., et al. (2012b). Antitumor agent calixarene 0118 targets human galectin-1 as an allosteric inhibitor of carbohydrate binding. *J. Med. Chem.* 55, 5121–5129. doi: 10.1021/jm300014q

Dings, R. P. M., Levine, J. I., Astorgues-Xerri, L., Kumar, N., Serova, M., Macdonald, J., et al. (2012a). 568 design of ptx008 that allosterically targets galectin-1 to inhibit tumor growth in mice. *Eur. J. Cancer* 48, 174–174. 10.1016/S0959-8049(12)72365-1 doi: 10.1016/S0959-8049(12)72365-1

Flink, S., and Reinhoudt, D. N. (1999). Recognition of cations by self-assembled monolayers of crown ethers. *J. Phys. Chem. B* 103, 6515–6520. doi: 10.1021/jp990014v

Gaeta, C., Talotta, C., Farina, F., Teixeira, F. A., Marcos, P. M., Ascenso, J. R., et al. (2012). Alkylammonium cation complexation into the narrow cavity of Dihomooxacalix [4] arene macrocycle. *J. Org. Chem.* 77, 10285–10293. doi: 10.1021/jo3019945

Geraci, C., Consoli, G. M., Galante, E., Bousquet, E., Pappalardo, M., and Spadaro, A. (2008). Calix[4]arene decorated with four Tn antigen glycomimetic units and P₃CS immunoadjuvant: synthesis, characterization, and anticancer immunological evaluation. *Bioconjugate Chem.* 19, 751–758. doi: 10.1021/bc700411w

Gómez-Machuca, H., Quiroga-Campano, C., Jullian, C., Fuente, J. D., Pessoa-Mahana, H., Escobar, C. A., et al. (2014). Study by fluorescence of calix[4]arenes bearing heterocycles with anions: highly selective detection of iodide. *J. Incl. Phenom. Macrocycl. Chem.* 80, 369–375. doi: 10.1007/s10847-014-0418-2

Granata, G., Paterniti, I., Geraci, C., Cunsolo, F., Esposito, E., Cordaro, M., et al. (2017). Potential eye drop based on a calix [4] arene nanoassembly for curcumin delivery: Enhanced drug solubility, stability, and anti-inflammatory effect. *Mol. Pharmacol.* 14, 1610–1622. doi: 10.1021/acs.molpharmaceut.6b01066

Guo, S., Song, Y., He, Y., Hu, X. Y., and Wang, L. (2018). Highly efficient artificial light-harvesting systems constructed in aqueous solution based on supramolecular self-assembly. *Angew Chem. Int. Ed.* 57, 3163–3167. doi: 10.1002/anie.201800175

Gutsche, C. D., Dhawan, B., No, K. H., and Muthukrishnan, R. (1981). Calixarenes. 4. The synthesis, characterization, and properties of the calixarenes from p-tert-butylphenol. *J. Am. Chem. Soc.* 103, 3782–3792. doi: 10.1021/ja00403a028

Harris, S. J. (1995). *Calixarene-Based Compounds Having Antibacterial, Antifungal, Anticancer-HIV Activity.* WO Patent No 95/19974. Geneva: World Intellectual Property Organization International Bureau.

Hu, X. Y., Zhang, P., Xuan, W., Wei, X., Xiao, T., Jiang, J., et al. (2012). Pillar[5]arene-based supramolecular polypseudorotaxanes constructed from quadruple hydrogen bonding. *Polymer Chem.* 3, 3060–3063. doi: 10.1039/c2py20285a

Hulíková, K., Grobárová, V., Krivohlavá, R., and Fišerová, A. (2010). Antitumor activity of N-acetyl-D- glucosamine-substituted glycoconjugates and combined therapy with keyhole limpet hemocyanin in B16F10 mouse melanoma model. *Folia Microbiol.* 55, 528–532. doi: 10.1007/s12223-010-0087-5

Hussain, M. A., Ashraf, M. U., Muhammad, G., Tahir, M. N., and Bukhari, S. N. A. (2017). Calixarene: a versatile material for drug design and applications. *Current Pharm. Design.* 23, 2377–2388. doi: 10.2174/1381612822666160928143328

Ji, S., Tang, S., Li, K., Li, Z., Liang, W., Qiao, X., et al. (2017). Licoricidin inhibits the growth of sw480 human colorectal adenocarcinoma cells, *in vitro*, and, *in vivo*, by inducing cycle arrest, apoptosis and autophagy. *Toxicol. Appl. Pharm.* 326, 25–33. doi: 10.1016/j.taap.2017.04.015

Kim, K., Selvapalam, N., Ko, Y. H., Park, K. M., Kim, D., and Kim, J. (2007). Functionalized cucurbiturils and their applications. *Cheminform* 36, 267–279. doi: 10.1039/B603088M

Koonce, N. A., Griffin, R. J., Dings, R. P. M. (2017). Galectin-1 inhibitor otx008 induces tumor vessel normalization and tumor growth inhibition in human head and neck squamous cell carcinoma models. *Int. J. Mol. Sci.* 18, 2671–2679. doi: 10.3390/ijms18122671

Kralj, M., Tusekbozić, L., and Frkanec, L. (2008). Biomedical potentials of crown ethers: prospective antitumor agents. *Chemmedchem* 3, 1478–1492. doi: 10.1002/cmdc.200800118

Läppchen, T., Dings, R. P. M., Rossin, R., Simon, J. F., Visser, T. J., Bakker, M., et al. (2015). Novel analogs of antitumor agent calixarene 0118: Synthesis, cytotoxicity, click labeling with 2-[18F] fluoroethylazide, and *in vivo* evaluation. *Eur. J. Med. Chem.* 89, 279–295. doi: 10.1016/j.ejmech.2014.10.048

Lee, J. W., Samal, S., Selvapalam, N., Kim, H. J., and Kim, K. (2003). Cucurbituril homologues and derivatives: new opportunities in supramolecular chemistry. *Cheminform* 34, 621–630. doi: 10.1021/ar020254k

Lehn, J. (1988). Supramolecular chemistry—scope and perspectives molecules, supermolecules, and molecular devices (nobel lecture). *Angew. Chem. Int. Ed.* 27, 89–112. doi: 10.1002/anie.198800891

Li, D. H., Hu, P., Xu, S. T., Fang, C. Y., Tang, S., Wang, X. Y., et al. (2017). Lasiokaurin derivatives: synthesis, antimicrobial and antitumor biological evaluation, and apoptosis-inducing effects. *Arch. Pharm. Res.* 40, 796–806. doi: 10.1007/s12272-016-0867-9

Liu, Y., Sun, J., and Yan, C. G. (2017). Synthesis and crystal structures of p-tert-butyldihomooxacalix [4] arene mono-Schiff bases. *J. Incl. Phenom. Macrocycl. Chem.* 87, 157–166. doi: 10.1007/s10847-016-0687-z

Liu, Y., Zhao, L. L., Sun, J., and Yan, C. G. (2018). Convenient synthesis and coordination properties of p-tert-butyldihomooxacalix[4]arene mono-schiff bases. *Polycycl. Aromat. Comp.* 5, 1–16. doi: 10.1080/10406638.2018.1469520

Ludwig, R., and Dzung, N. T. K. (2002). Calixarene-based molecules for cation recognition. *Sensors* 22, 397–416. doi: 10.3390/s21000397

Marcos, P. M., Félix, S., Ascenso, J. R., Segurado, M. A., Mellah, B., Abidi, R., et al. (2006). Complexation and transport of alkali and alkaline earth metal cations by p-tert-butyldihomooxacalix [4] arene tetraketone derivatives: erratum. *Supramol. Chem.* 18, 285–297. doi: 10.1080/106102706007 73006

Marcos, P. M., Teixeira, F. A., Segurado, M. A., Ascenso, J. R., Bernardino, R. J., Michel, S., et al. (2014). Bidentate urea derivatives of p-tert-butyldihomooxacalix [4] arene: neutral receptors for anion complexation. *J. Org. Chem.* 79, 742–751. doi: 10.1021/jo4026012

Motornaya, A. E., Alimbarova, L. M., Shokova, E. A., and Kovalev, V. V. (2006). Synthesis and antiherpetic activity of N-(3-amino-1-adamantyl) calix [4] arenes. *Pharm. Chem. J.* 40, 68–72. doi: 10.1007/s11094-006-0060-4

Mourer, M., Psychogios, N., Laumond, G., Aubertin, A. M., and Regnouf-de-Vains, J. B. (2010). Synthesis and anti-HIV evaluation of water-soluble calixarene-based bithiazolyl podands. *Bioorg. Med. Chem.* 18, 36–45. doi: 10.1016/j.bmc.2009.11.016

Muneer, S., Memon, S., Pahnwar, Q. K., Bhatti, A. A., and Khokhar, T. S. (2017). Synthesis and investigation of antimicrobial properties of pyrrolidine appended calix [4] arene. *J. Anal. Sci. Technol.* 8, 3–8. doi: 10.1186/s40543-017-0111-3

Mutihac, L., Lee, J. H., Kim, J. S., and Vicen, J. (2011). Recognition of amino acids by functionalized calixarenes. *Chem. Soc. Rev.* 40, 2777–2796. doi: 10.1039/c0cs00005a

Naseer, M. M., Ahmed, M., and Hameed, S. (2017). Functionalized calix[4]arenes as potential therapeutic agents, *Chem. Biol. Drug Des.* 89, 243–256. doi: 10.1111/cbdd.12818

Nasuhi Pur, F., and Dilmaghani, K. A. (2014). Calixplatin: novel potential anticancer agent based on the platinum complex with functionalized calixarene. *J. Coord. Chem.* 67, 440–448. doi: 10.1080/00958972.2014. 890718

Neagu, M., Ion, R. M., Manda, G., Constantin, C., Radu, E., and Cristu, Z. (2010). Antitumoral effect of calixarenes in experimental photodynamic therapy with K562 tumor cell line. *Rom. J. Biochem.* 47, 17–35.

Patra, S., Boricha, V. P., and Paul, P. (2019). Dual-mode calixarene-based chemosensor: highly selective fluorogenic detection of Hg^{2+} and chromogenic detection of Cu^{2+} with a single ionophore. *Eur. J. Inorg. Chem.* 2019, 199–205. doi: 10.1002/ejic.201800925

Paz, H., Joo, E. J., Chou, C. H., Fei, F., Mayo, K. H., and Abdel-Azim, H. (2018). Treatment of B-cell precursor acute lymphoblastic leukemia with the Galectin-1 inhibitor PTX008. *J. Exp. Clin. Cancer Res.* 37, 67–91. doi: 10.1186/s13046-018-0721-7

Pelizzarorocha, K. J., de Jesus, M. B., Rueladesousa, R. R., Nakamura, C. V., Reis, F. S., de Fátima A, et al. (2013). Calix[6]arene bypasses human pancreatic cancer aggressiveness: downregulation of receptor tyrosine kinases and induction of cell death by reticulum stress and autophagy. *Biochim Biophys Acta.* 1833, 2856–2865. doi: 10.1016/j.bbamcr.2013.07.010

Quan, H., Liu, H., Li, C., and Lou, L. (2009). 1,4-diamino-2,3-dicyano-1,4-bis(methylthio)butadiene (u0126) enhances the cytotoxicity of combretastatin a4 independently of mitogen-activated protein kinase kinase. *J. Pharmacol. Exp. Ther.* 330, 326–333. doi: 10.1124/jpet.109.153320

Sansone, F., Baldini, L., Casnati, A., and Ungaro, R. (2008). Conformationally mobile glucosylthioureidocalix [6]-and calix[8]arenes: Synthesis, aggregation and lectin binding. *Supramol. Chem.* 20, 161–168. doi: 10.1080/10610270701777344

Shah, R. B., Valand, N. N., Sutariya, P. G., and Menon, S. K. (2016). Design, synthesis and characterization of quinoline–pyrimidine linked calix [4] arene scaffolds as anti-malarial agents. *J. Inclusion Phenom. Macro. Chem.* 84, 173–178. doi: 10.1007/s10847-015-0581-0

Sheldrick, G. M. (1997). *SHELXS-97 and SHELXL-97.* Gottingen: University of Gottingen.

Soares, M. N. Jr., Gáscon, T. M., Fonseca, F. L., Ferreira, K. S., and Bagatin, I. A. (2014). Evaluation of the biological effects of 5-Cl-8-oxyquinolinepropoxycalix [4] arene and 8-oxyquinolinepropoxycalix [4] arene *in vitro* and *in vivo. J. Mater. Sci. Eng. C-Mater.* 40, 260–266. doi: 10.1016/j.msec.2014.04.002

Stella, V. J., and He, Q. (2008). Cyclodextrins. *Toxicol. Pathol.* 36, 30–42. doi: 10.1177/0192623307310945

Sun, G., Pu, L., Pangannaya, S., Xiao, T., Hu, X. Y., Jiang, J., et al. (2019). β-D-galactose-functionalized pillar [5] arene with interesting planar-chirality for constructing chiral nanoparticles. *Front. Chem.* 7:743. doi: 10.3389/fchem.2019.00743

Sun, J., Liu, D. M., Wang, J. X., and Yan, C. G. (2009a). Regioselective synthesis of calix [4] arene 1, 3-di-and monosubstituted sulfur-containing Schiff bases. *J. Incl. Phenom. Macro. Chem.* 64, 317–324. doi: 10.1007/s10847-009-9570-5

Sun, J., Liu, D. M., and Yan, C. G. (2009b). Transition metal complexes of bidentate p-tert-butylcalix [4] arene S-alkyldithio carbazate Schiff bases. *J. Coord. Chem.* 62, 2337–2346. doi: 10.1080/00958970902818208

Sun, S., Geng, M., Huang, L., Chen, Y., and Yao, Y. (2018). A new amphiphilic pillar[5]arene: synthesis, controllable self-assembly in water and application in white-light-emitting system. *Chem. Commun* 54, 13006–13009. doi: 10.1039/C8CC07658H

Talotta, C., Gaeta, C., De Rosa, M., Ascenso, J. R., Marcos, P. M., and Neri, P. (2016). Alkylammonium guest induced-fit Recognition by a flexible dihomooxacalix [4] arene derivative. *Eur. J. Org. Chem.* 2016, 158–167. doi: 10.1002/ejoc.201501319

Valle, E. M. M. D. (2004). Cyclodextrins and their uses: a review. *Process Biochem.* 39, 1033–1046. doi: 10.1016/S0032-9592(03)00258-9

Viola, S., Consoli, G. M., Merlo, S., Drago, F., Sortino, M. A., and Geraci, C. (2010a). Inhibition of rat glioma cell migration and proliferation by a calix[8]arene scaffold exposing multiple glcnac and ureido functionalities. *Neuro.Chem.* 107, 1047–1055. doi: 10.1111/j.1471-4159.2008. 05656.x

Viola, S., Merlo, S., Consoli, G. M., Drago, F., Geraci, C., and Sortino, M. A. (2010b). Modulation of C6 glioma cell proliferation by ureido-calix[8]arenes. *Pharmacology* 3, 182–188. doi: 10.1159/000317518

Yokoyama, T., and Mizuguchi, M. (2019). Crown ethers as transthyretin amyloidogenesis inhibitors. *J. Med. Chem.* 62, 2076–2082. doi: 10.1021/acs.jmedchem.8b01700

Yousaf, A., Hamid, S. A., Bunnori, N. M., and Ishola, A. A. (2015). Applications of calixarenes in cancer chemotherapy: facts and perspectives. *Drug Design, Dev. Therapy.* 9, 2831–2838. doi: 10.2147/DDDT.S83213

Zadmard, R., and Alavijeh, N. S. (2014). Protein surface recognition by calixarenes. *RSC Advances* 4, 41529–41542. doi: 10.1039/C4RA 05181E

Zhang, R., Wang, C., Long, R., Chen, T., Yan, C., and Yao, Y. (2019). Pillar[5]arene based [1]rotaxane systems with redox-responsive host-guest property: design, synthesis and the key role of chain length. *Front. Chem.* 7:508. doi: 10.3389/fchem.2019.00508

Zhang, Y. M., Xu, Q. Y., and Liu, Y. (2019). Molecular recognition and biological application of modified β-cyclodextrins. *Sci. Chin.* 62, 1–12. doi: 10.1007/s11426-018-9405-3

Zhou, H., Wang, D. A., Baldini, L., Ennis, E., Jain, R., Carie, A., et al. (2006). Structure-activity studies on a library of potent calix[4]arene-based PDGF antagonists that inhibit PDGF-stimulated PDGFR tyrosine phosphorylation. *Org. Biomol. Chem.* 4, 2376–2386. doi: 10.1039/B5 15483A

Zhou, J., Yu, G., and Huang, F. (2017). Supramolecular chemotherapy based on host–guest molecular recognition: a novel strategy in the battle against cancer with a bright future. *Chem. Soc. Rev.* 46, 7021–7053. doi: 10.1039/C6CS00898D